Development of a Cervical Spine Model for Rear Impact Conditions

Undergraduate Honors Thesis

Presented in Partial Fulfillment of the Requirements for

Graduation with Distinction

at The Ohio State University

By

Michael J. Keller

* * * * *

The Ohio State University

2010

Defense Committee:

Dr. John H. Bolte IV, Advisor

Dr. Rebecca Dupaix

Approved by

Advisor

Undergraduate Program in Mechanical Engineering

Copyrighted by

Michael J. Keller

2010

To my mom and dad and in memory of my grandma,

Thank you for your love, support, and

the sacrifices you made to provide me with the best education.

Abstract

The cost of automobile accidents is high to both individuals and society. In 2006, approximately 43,000 people were killed in car accidents and 2,575,000 more were injured. Rear impact collisions alone accounted for 740,000 neck injuries, most associated with whiplash, carrying a total cost of $8 billion. Whiplash remains a challenging problem because injury mechanisms are poorly understood; however, studying detailed intervertebral kinematics can provide valuable insight into possible mechanisms. Currently, The Ohio State University Injury Biomechanics Research Laboratory is involved in research studies to examine detailed intervertebral kinematics by testing post mortem human subjects (PMHS) in varying speed rear impact collisions. However, experimental tests with PMHS are limited because they are very expensive, subjects are hard to obtain, and too few tests are run for statistical significance. The development of an accurate cervical spine model would help to overcome these limitations. Therefore, the purpose of this study is to develop a constrained, 2-D flexion-extension model of the cervical spine and head that is appropriate for use in low to moderate speed rear impact collisions.

To achieve this goal, ADAMS, a simulation tool for multibody dynamics, was used to develop the model. Geometry for the model was obtained from an actual cervical spine specimen using 3-D reconstruction techniques. The solid body geometry was

constrained by applying ligaments, approximated as linear spring/damper elements, and non-linear intervertebral discs. The model was simulated by directly applying T1 kinematics from experimental testing directly to T1 of the model. Validation was performed by comparing head kinematics from the model and experimental response.

In the low speed simulation, acceleration validation results matched well except for a ~10 ms lead in the model response and accurately predicted head displacements. In the moderate speed simulation, error and lead time increased significantly, resulting in less accurate head displacements.

Acknowledgements

This study could not have been completed without the support of many individuals. First and foremost, thank you to my advisor Dr. John Bolte IV for welcoming me into his lab and allowing me to work on this study. Thank you for your continual support, encouragement, patience, and providing me with all the resources I needed to get the job done.

Thank you to Yun-Seok Kang who was the driving force behind this study. Yun taught me everything I needed to know about the cervical spine, rear impact, and modeling with ADAMS. Thank you for your huge commitment of time and patience. It was a pleasure working with you on a daily basis.

Thank you to Greg Knapik of The Ohio State University Biodynamics Laboratory. Greg played a critical role in helping me overcome the obstacles I experienced with solid geometry creation. Greg generously offered his expertise, time, and software to help me get the results I needed. Greg also provided the skull for my model.

Finally, thank you to all the students of the OSU IBRL. Thank you to Mandy Agnew, Matt Long, Matt Kremer, Hannah Gustafson, Kyle Icke, Brian Suntay, Julie Bing, and Tony Vergis. Thank you for your willingness to always lend a helping hand and for making every day in the lab a fun experience.

Table of Contents

Page

List of Figures

Figure Page

List of Tables

Table Page

Chapter 1

Introduction

1.1 Motivation

Despite its convenience and usefulness, the automobile presents a serious problem in the form of motor vehicle crashes. In 2006, approximately 43,000 people were killed in such accidents and 2,575,000 more were injured. Furthermore, it was reported that of these injuries rear impact collisions accounted for 740,000 neck injuries, most associated with whiplash [1]. Although whiplash is classified as a minor injury, its associated costs to both individuals and society are significant, approximately $8 billion annually [2]. It has been documented in insurance claims that 70% of all bodily injury claims and 43% of medical costs are due to whiplash injuries [3].

Whiplash is a challenging injury to examine because evidence of injury and injury mechanisms are poorly defined and understood. It is an injury to the soft tissues of the neck that occurs most often in rear impact collisions. The inertia of the head causes it to lag in response to an external force in the same frame of reference. This creates a movement differential between the head and torso which causes injury [4]. In many whiplash cases, patients complain of neck pain but no objective evidence of injury is present in x-ray, CT, or MRI. The lack of objective evidence does not conclude that

injury is not present; rather it reflects the inability of current methods to detect injury. This leads to patient frustration since clinical professionals are reluctant to diagnose injury without substantial proof. Clinicians can make false assumptions that the patient is malingering or their pain is mental, thus they are left untreated [5].

The precise location of whiplash injury is debated in literature; however, there is agreement that the injury occurs due to relative rotation and displacement between adjacent vertebrae that exceeds the physiological range of motion. Based on this knowledge, obtaining detailed cervical spine kinematics during a rear impact collision provides valuable insight into possible injury mechanisms and a more confident diagnosis of whiplash injury [6]. To analyze cervical spine kinematics, past and current studies have obtained data from human volunteers and post mortem human subjects (PMHS) in simulated rear impact conditions. However, these studies are often limited in their application and analysis. To overcome these limitations, experimentally validated models based on accurate geometry, soft tissue properties, boundary conditions, and loading conditions can be a promising alternative [7]. The goal of the current research is to develop a validated model that can address the limitations inherent to PMHS testing.

1.2 Experimental Work

Several studies have investigated cervical spine biomechanics and injury mechanisms in simulated rear impacts using PMHS.

In a study conducted by Deng et al. [8] in 2000, 26 simulated low speed rear impacts were performed on six PMHS. Neck targets were implanted at each cervical level and high speed x-ray was used to measure linear and angular displacements

between adjacent vertebrae. Head kinematics were obtained using a nine accelerometer mount fixed to the apex of the head. Data were processed by differentiating the linear and angular displacements to find velocities and accelerations.

The study performed by Deng et al. [8] had several limitations despite providing a minimally invasive and visually appealing way to investigate intervertebral kinematics in PMHS. First, high speed x-ray is limited by a small field of view and acquisition rate. The field of view and acquisition rate for this study were limited to 25 cm x 25 cm and 250 frames/sec, respectively. Consequently, high speed x-ray is only useful for low speed conditions. Finally, the presence of noise in experimental data makes obtaining velocities and accelerations through numerical differentiation challenging and adversely affects inverse dynamic calculations.

Panjabi et al. [9] [10] conducted two studies to examine detailed intervertebral kinematics using isolated cervical spine specimens. In both studies, the muscles and skin were removed from the specimen to evaluate the ligamentous spine. Additionally, the 2005 test also incorporated a spring-cable system to replicate muscle forces. The specimen was mounted to a mini-sled and a horizontal acceleration was applied to simulate a rear impact. Markers at each vertebral level along with high speed video were used to obtain kinematic data.

Similar to high speed x-ray, these studies were limited in their application due to the relatively low acquisition rate of high speed video (approximately 1000 frames/sec). Furthermore, mounting the isolated cervical spine to a sled produced inaccurate boundary conditions. In rear impact scenarios, the rotation of the thorax is crucial to cervical spine

kinematics. In these studies, the thorax was fixed to the sled, therefore eliminating its contributions to intervertebral motion. Additionally, these studies removed the skin and muscles from the cervical spine which weakens the structure and can lead to overestimation of injury.

A study performed by Yoganandan et al. [11] addressed the boundary condition issues inherent to Panjabi's work. Five PMHS were placed on a sled and subjected to simulated rear impacts. High speed video cameras captured gross kinematics from photo targets placed on the head, first thoracic vertebrae (T1), iliac crest, and sacrum. However, this study was limited in that it only measured gross kinematics, defined as relative motion between the head and T1.

A study performed by Berthelon et al. [12] was the first to use angular rate sensors and accelerometers to measure detailed intervertebral kinematics. Instrumentation was attached to the anterior aspect of the second and fifth cervical vertebrae (C2 and C5) and T1 of three PMHS. An air piston propelled sled simulated a rear impact condition. The new instrumentation solved the low sampling rate issue inherent to high speed x-ray and video. However, the study was limited in that it only measured partial intervertebral kinematics of the cervical spine (i.e. C2 and C5 only).

The Injury Biomechanics Research Laboratory (IBRL) at The Ohio State University is currently involved in PMHS testing to evaluate detailed intervertebral kinematics of the cervical spine in simulated, varying speed rear impact collisions. The goal of the work is to evaluate the kinematic response of PMHS compared to three rear impact dummies currently being used by car manufacturers as safety testing tools. The

testing utilizes a new technique for instrumenting the cervical spine which does not damage the structural integrity of surrounding soft tissue. The anterior aspect of each cervical vertebra, with the exception of C1 (due to its small size), and T1 are instrumented with accelerometers and angular rate sensors. A configuration of six accelerometers and three angular rate sensors are fixed to the head to measure accurate head kinematics. This is the first study to examine detailed intervertebral kinematics at every vertebral level using accelerometers and angular rate sensors.

The study currently being conducted at the IBRL has addressed several limitations of past studies; however, the work still suffers from the restrictions inherent to all PMHS testing. PMHS testing is challenging and requires a large investment of time, resources, money, and labor to perform one trial. Furthermore, PMHS for testing are scarce and some must be rejected because they do not meet the testing criteria. As a result, too few tests are run for a particular study to achieve statistical significance. Experimental work may adversely affect vertebral dynamics by introducing the risk of soft tissue damage during instrumentation. Furthermore, attaching instrumentation directly to the vertebrae can change its dynamic response. In response to these limitations, accurate models can help to fill the gap.

1.3 Advantages of Models

An accurate model can supplement experimental work with PMHS that is costly, time consuming, and labor intensive. Running a simulation takes very little time and parameters such as design variables, input conditions, and boundary conditions can be changed quickly and easily. This allows for a wider range of test conditions and

scenarios to be examined. Several important parameters can be derived from simulation results such as displacements, linear accelerations, and angular accelerations. Finally, experiments are limited in that they only describe external responses of the spine. Models not only solve for external response but provide detailed information about the internal response such as local deformation, stress, strain, and load sharing [7]. Internal responses are crucial for gaining insight into the mechanisms of whiplash injury.

1.4 Modeling Fundamentals

For a model to be useful in determining cervical spine biomechanics, four aspects are critical to its development [13]:

1. Accurate geometry- Surface geometry and the major components of the cervical spine greatly influence motion and biomechanical response; therefore, a more accurate representation is preferred. Furthermore, anatomically accurate vertebrae provide anatomical landmarks for the connection of ligaments and discs. CT or laser scanning methods are useful tools for 3-D reconstructions of cervical anatomy.
2. Accurate material properties- The material properties of the hard and soft tissue of the cervical spine greatly influence biomechanical response. However, consistent data regarding cervical spine soft tissue properties does not currently exist. This is due to the rate dependent nature of biological tissues, large variation among subjects, difficulty of testing, and the drawbacks of *ex vivo* testing.
3. Boundary conditions- For a model to accurately represent *in vivo* responses, proper boundary conditions must be defined. With regards to the cervical spine,

kinematic response is greatly influenced by T1 motion; therefore, a boundary condition must be applied to the superior end of the model to account for T1 interaction. A free boundary condition is typical for the head.

4. Validation- A model is worthless without being properly validated using experimental data. Validation is typically done by comparing kinematic data (e.g. linear accelerations, angular accelerations, displacements) from the model and experimental tests.

1.5 Previously Developed Cervical Spine Models

Several studies have developed computerized cervical spine models, primarily focused on using finite element modeling (FEM).

Kleinberger [14] developed a three dimensional FEM of the cervical spine. The model included all the cervical vertebrae (C1-C7), T1, the intervertebral discs, relevant spinal ligaments, and a rigid head. The vertebrae were generated from a mesh and included all important structures such as the vertebral body, articular facets, laminae, spinous process, pedicles, and transverse processes. Intervertebral discs, facet joints, and spinal ligaments were approximated as linear elastic materials. The model included the anterior and posterior longitudinal ligaments (ALL and PLL), ligamentum flavum (LF), supraspinous ligament (SSL), and capsular ligaments (CL). The surfaces between the discs and vertebral bodies were defined as tied interfaces and a pivot joint was placed between the occipital condyle of the skull and C1.

Three simulations were run with the model and validated using experimental data from literature. Axial compression was simulated by fixing T1 and imposing a pressure

ramp on the planar surface of the occipital condyles. Total displacement and axial stiffness agreed well with literature. A second simulation tested large strain responses of the model by imposing a 10 mm displacement on C1. Gross vertebral kinematics and spine deformation shapes also were consistent with literature. Finally, an 8g frontal crash was simulated by applying a velocity profile to T1 in the –x direction. The model accurately predicted head lag and neck rotation as previously observed in volunteer and PMHS testing [14]. Despite comparing well with experimental data, the model used several simplifying assumptions, most notably the characterization of intervertebral discs and ligaments as isotropic linear elements and the approximation of the atlanto-occipital joint as a pivot joint.

Dauviliers et al. [15] developed a cervical spine model for simulating frontal and lateral impacts. The head and vertebrae, C1 through T1, were included and modeled as rigid bodies. To reduce the number of model elements, components of the vertebrae were limited to the vertebral body, facet joints, laminae, spinous process, pedicles, and transverse processes. Vertebral orientations were obtained from x-ray images of PMHS spines. Due to their complexity, the atlanto-occipital and atlanto-axial joints were modeled as spherical joints that allowed for axial rotation, flexion, and extension. Intervertebral discs, facet joints, and spinal ligaments were modeled as viscoelastic spring-damper elements defined by a stiffness and damping coefficient. The spinal ligaments considered for the model were the ALL, PLL, LF, SSL, and interspinous ligament (ISL).

The model explained above was validated by applying the same linear accelerations to T1 as previously obtained in volunteer testing and comparing the

response of the head in the model (i.e. displacements, linear accelerations, angular accelerations) with volunteer responses. With the exception of z-displacement in frontal impact, model and volunteer responses matched well.

A finite element model of the cervical spine was developed by Yang et al. [16] and included the skull, C1 through T1, intervertebral discs, and spinal ligaments. Neck geometry was constructed from an MRI of a 50^{th} percentile male. As an improvement over existing models, the vertebrae were modeled as linear elastic materials and the intervertebral discs as linear viscoelastic materials. The model also included more spinal ligaments, especially in the upper cervical spine, such as the alar ligaments, transverse ligament, and the anterior/posterior atlanto-occipital membrane. All ligaments were modeled as non-linear bar elements that worked in tension only. The passive effects of the neck muscles were also modeled in a similar fashion to the ligaments. Synovial facet joint articulation was modeled by a sliding contact joint.

Data from head drop tests and simulated rear impact sled tests were used for model validation. For the head drop tests, head and neck loads and head acceleration were used for comparison. Head accelerations and global neck kinematics were compared for the sled test. This model developed by Yang et al. greatly improved on Kleinberger's model by including more complicated vertebral geometry, including more ligaments in the upper cervical spine, using non-linear ligament properties, modeling vertebrae as linear elastic bodies, including passive muscle effects, and including facet joint articulation.

This study plans to develop a new cervical spine model to address limitations and omissions of previous studies. For example, Kleinberger's model [14] was not validated for rear impact conditions. Furthermore, the approximation of the atlanto-occipital joint as a pivot joint was grossly inaccurate. The model developed by Dauviliers et al. [15] was only validated for frontal and lateral impact. While the Yang et al. model [16] was validated for rear impact, input conditions were at much different speeds than investigated for this study. The current study is most interested in analyzing gross kinematics of the cervical spine, a strength of the ADAMS environment. However, all previous models discussed utilized finite element models which focus more on highly localized stress and strain rather than gross kinematics.

1.6 Modeling with ADAMS

The model described in this study will be developed using ADAMS (MSC Software, 2010), a simulation tool that is used for analyzing multibody dynamics and complex motion. It differs from finite element modeling and has several advantages and disadvantages compared to those types of models. For example, ADAMS is excellent for analyzing gross kinematics of the cervical spine, the main focus of this study. Compared to finite element modeling, it is much better at handling large motions and highly non-linear behavior. On the other hand, finite element models can compute highly localized stress and strain values for soft tissues, discs, and vertebrae. The identification of localized stresses and strain is important for evaluating injury. ADAMS can do this on a much smaller scale using the force and displacement of model elements; however, the values are more general and not localized.

A model in ADAMS is easier to develop and requires fewer known inputs, an important advantage considering the inconsistency or lack of well documented cervical spine geometry and properties. Furthermore, input variables are easier to adjust in ADAMS and a simulation can be run in a fraction of the time and computing power needed for finite element.

Due to its strength in multibody dynamics, ease of use, reduction in input variables, and reduction in computing time, ADAMS was chosen to be most appropriate for this study. Furthermore, the study is focused on evaluating the gross kinematics of the cervical spine, a strength of the ADAMS environment. The results can be easily transferred to a finite element model in future work.

1.7 Project Objectives

Due to the limitations of experimental work and the advantages of accurate, validated models, a cervical spine model is developed to supplement experimental rear impact testing in the IBRL at The Ohio State University. The specific objectives of this study are:

1. Develop a constrained, 2-D flexion-extension model of the cervical spine and head in ADAMS that is appropriate for use in low to moderate speed rear impact simulations.
2. Validate the flexion-extension model by comparing head kinematics of the model and experimental data using T1 experimental kinematics as the model input.

Chapter 2

Anatomy

2.1 Cervical Vertebrae

The cervical spine (Figure 1), serves to protect the spinal cord, support the skull, and allow for a wide range of head movements. It consists of seven cervical vertebrae (C1 through C7) that are articulated by ligaments, discs, muscles, and tendons. The skull sits superior to the cervical spine while the thoracic spine sits inferior (Figure 2).

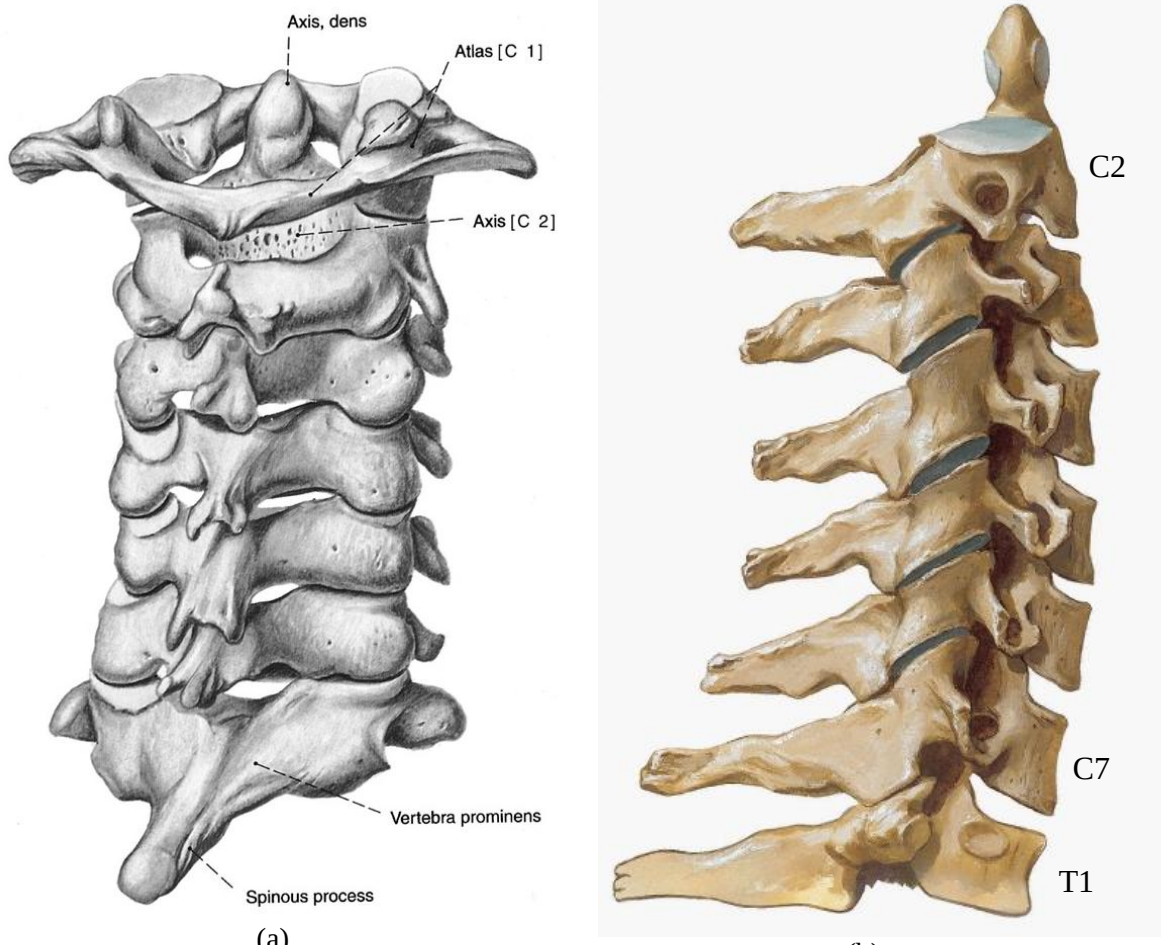

(a) (b)

Figure 1: Posterior oblique view (a) [18] and right lateral view (b) [19] of the cervical spine with C1 removed and T1 included.

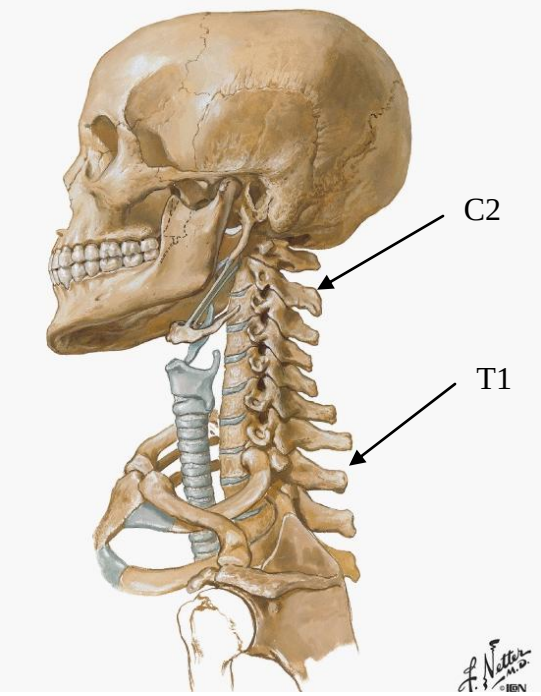

Figure 2: Right lateral view of the cervical spine with surrounding anatomy [19].

The vertebrae of the lower cervical spine, C3 through C7, share a similar morphology (Figure 3). The vertebral body, located anteriorly, supports body weight and provides strength to the spine. The vertebral arch, located posteriorly, is formed by the pedicles and laminae which come together to form the boundaries of the vertebral foramen. In the articulated spine, the vertebral foramina form a vertebral canal which houses and protects the spinal cord.

Seven processes extend from the vertebral arch and serve as soft tissue attachment sites. The spinous process, less prominent in most cervical vertebrae, extends posteriorly from the vertebral arch while two transverse processes extend laterally. C7, also referred to as vertebra prominens, is so called because it has a more prominent spinous process

(Figure 4). The articular processes of typical cervical vertebrae contain inferior and superior facets that articulate with adjacent vertebrae at approximately 45^{o} in the superior direction from the transverse plane [17] [18].

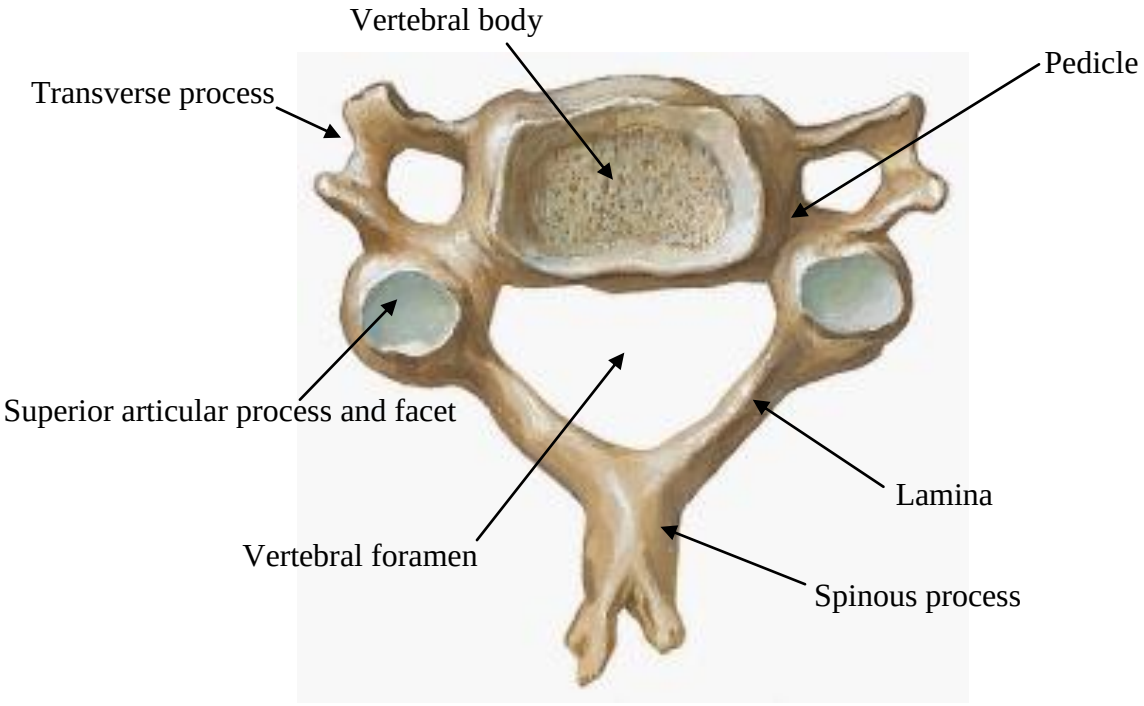

Figure 3: Superior view of a typical cervical vertebra [19].

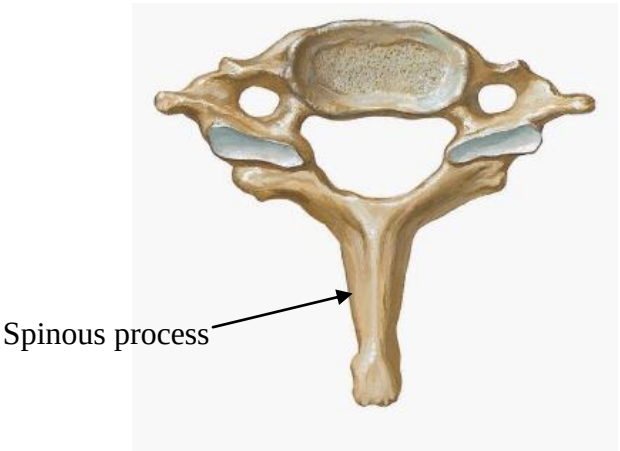

Figure 4: Superior view of C7 [19].

The first thoracic vertebra, T1, is often included in discussions of the cervical spine because its motion greatly influences kinematics of the cervical spine. It has morphology similar to C7 except it is larger in size, has a larger spinous process, does not have transverse foramina, and articulates with the first thoracic rib.

The vertebrae of the upper cervical spine, C1 and C2, have a significantly different morphology than the lower cervical spine. C1, also known as the atlas has an elliptical shape with no vertebral body, no spinous process, a large transverse process, and a large vertebral foramen (Figure 5). The atlas contains concave superior facets that articulate with the occipital condyles of the skull and relatively flat inferior facets that articulate with the superior facets of C2. C2, also known as the axis has a more typical structure except for the odontoid process, or dens, which projects superiorly from the vertebral body and provides an axis about which the atlas can rotate (Figure 6) [17].

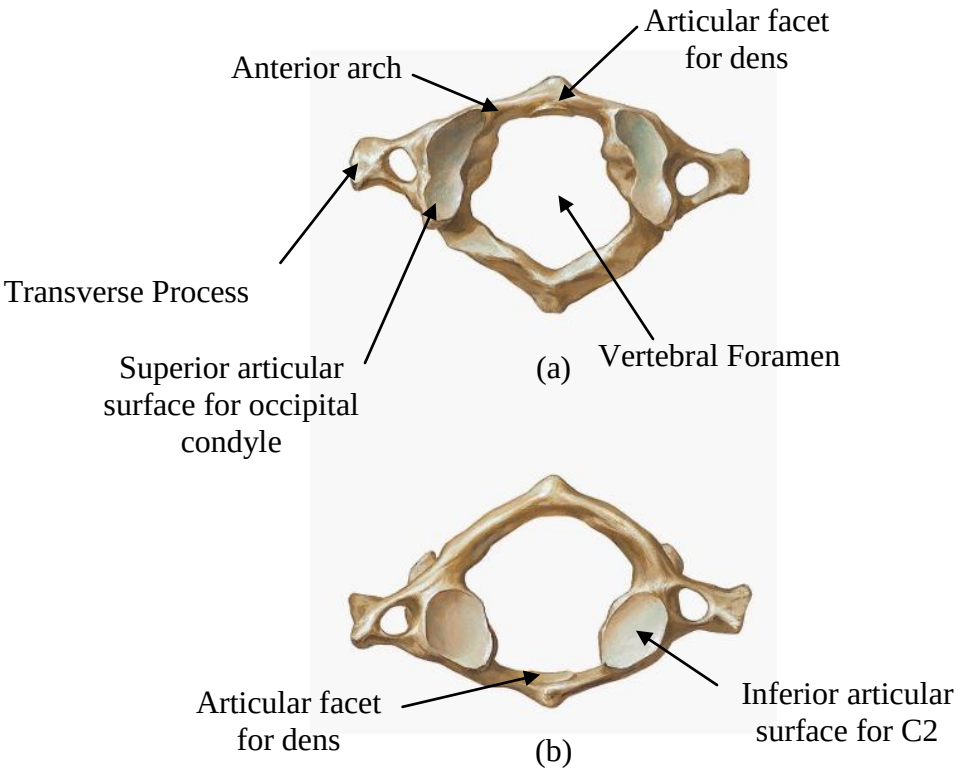

Figure 5: Superior view (a) and inferior view (b) of C1 [19].

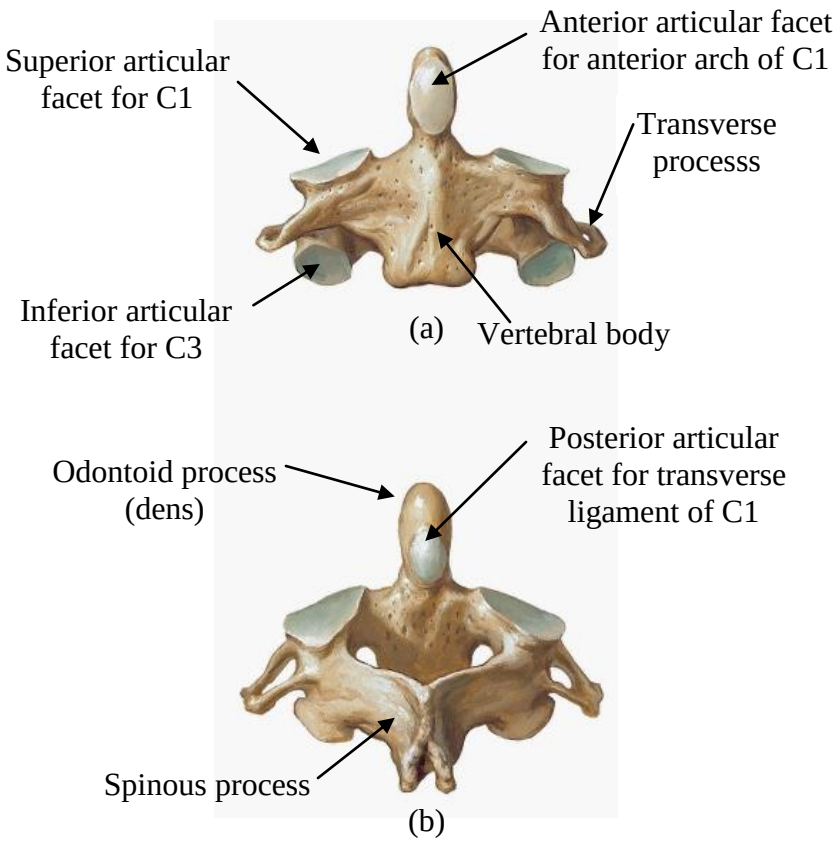

Figure 6: Anterior view (a) and posterior view (b) of C2 [19].

2.2 Ligaments, Discs, and Articulations

In the upper cervical spine, the occipital condyles of the skull (Figure 7) articulate with the superior facets of the atlas to form the atlanto-occipital joint. The free movement of this joint allows for flexion and extension of the head. The inferior facets of the atlas articulate with the superior facets of the axis to form the atlanto-axial joint which allows for axial rotation of the head [14]. The anterior surface of the dens articulates with the posterior surface of the anterior arch of the atlas and is held together by a number of ligaments [17].

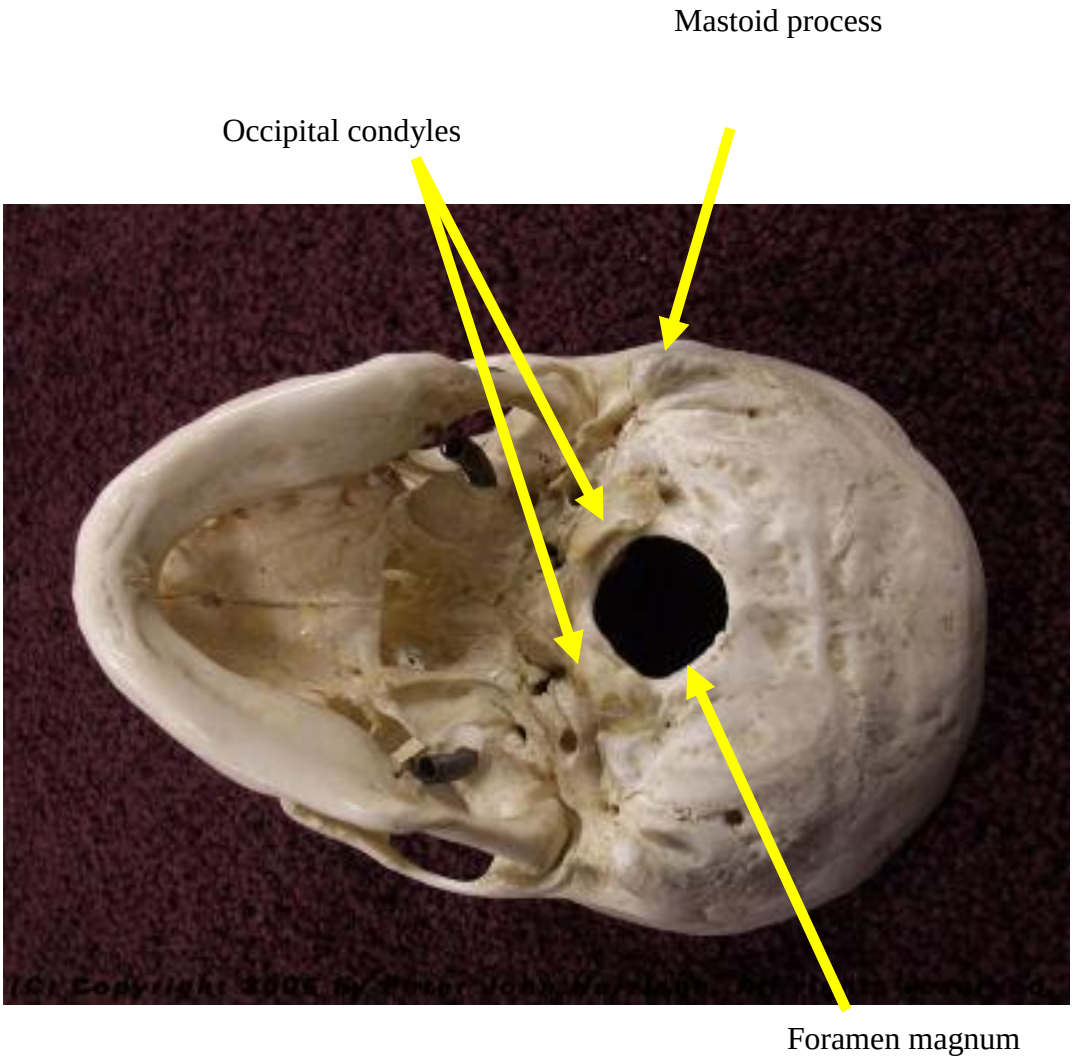

Figure 7: Inferior view of the skull.

Ligaments are viscoelastic in nature and work in tension to limit the range of motion of the spine [7]. The atlanto-occipital membrane (Figure 8) has anterior and posterior sections and connects C1 and the outer edge of the foramen magnum (Figure 7). The tectorial membrane connects the midline of the posterior aspect of the body of C2 to the anterior edge of the foramen magnum (Figure 9). Deeper ligaments include the cruciate ligament, apical ligament, and alar ligament. The cruciate ligament connects the dens to the arch of C1 and the anterior foramen magnum and provides stabilization for the upper cervical spine and helps maintain the articulation between the dens and C1 (Figure 10). Both the alar and apical ligaments work to hold the dens in place (Figure 11). The apical ligament connects the apex of the dens to the posterior edge of the foramen magnum. The alar ligament connects the apex of the dens to the lateral edges of the foramen magnum. The transverse ligament wraps around the dens and helps to maintain its stable articulation with C1 (Figure 12) [18].

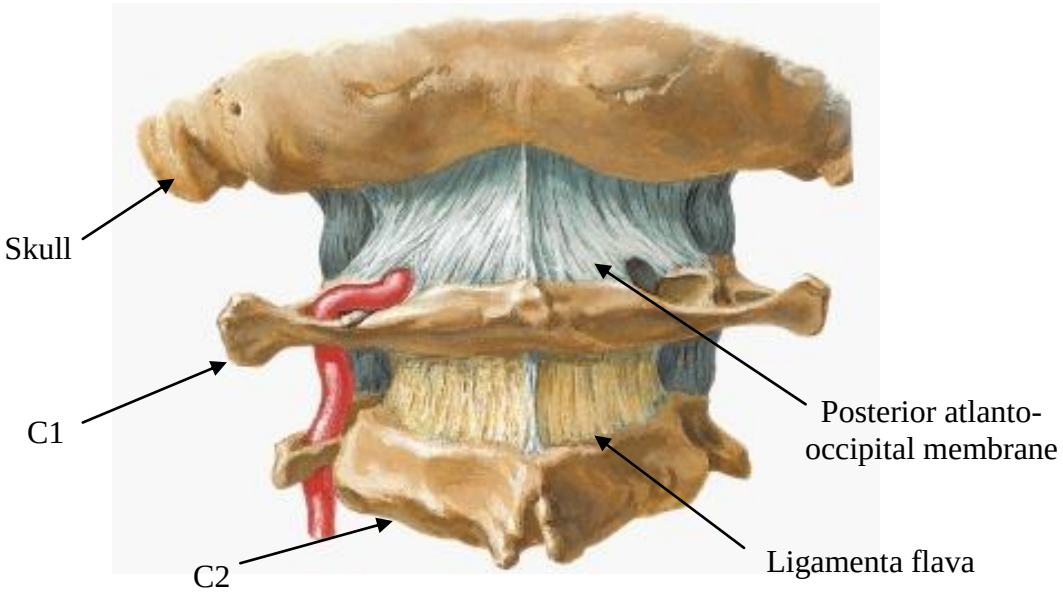

Figure 8: Posterior view of the upper cervical spine [19].

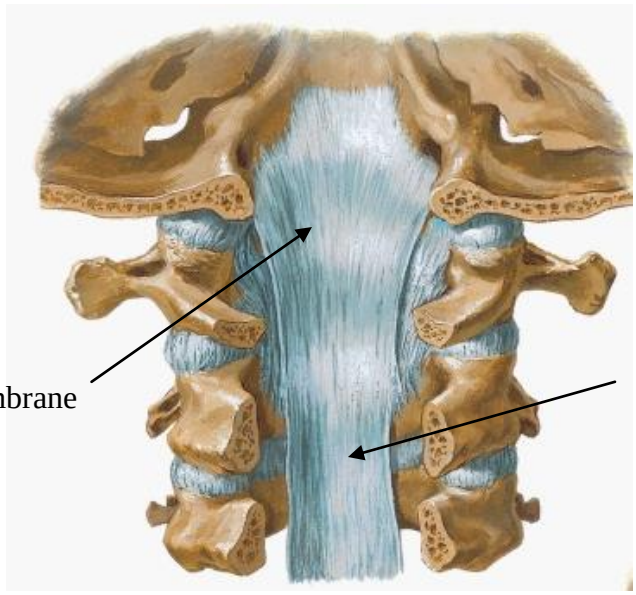

Figure 9: Posterior view of the upper cervical spine with posterior elements removed to expose ligaments on the posterior vertebral bodies [19].

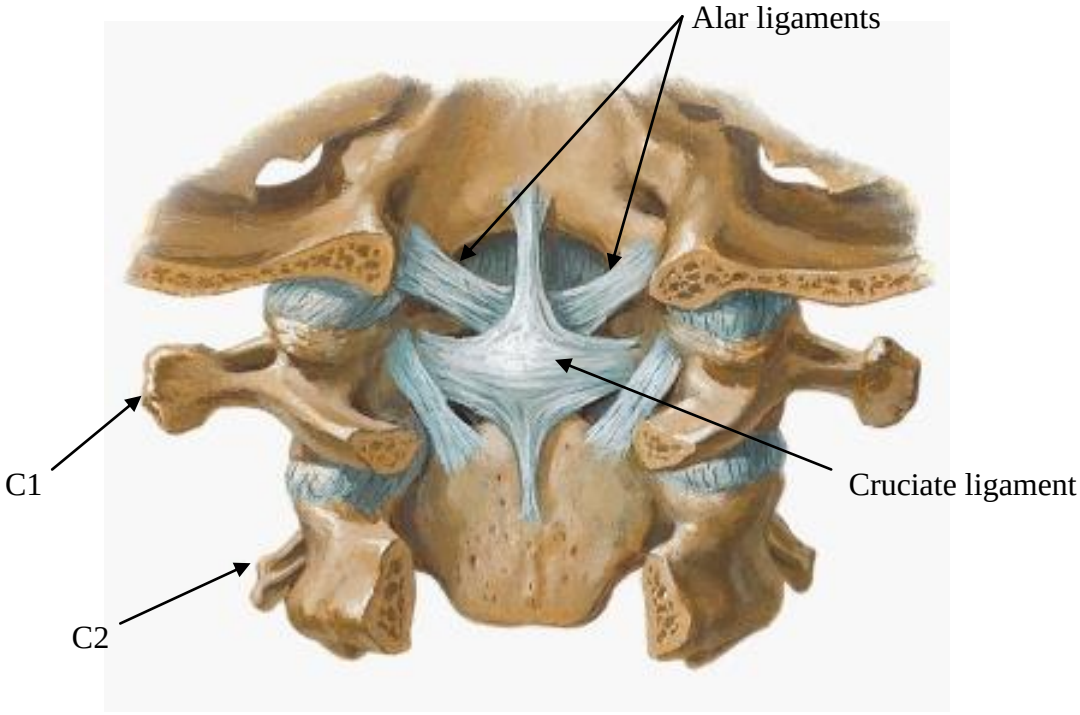

Figure 10: Posterior view of the upper cervical spine with posterior elements and the tectorial membrane removed to expose deeper ligaments [19].

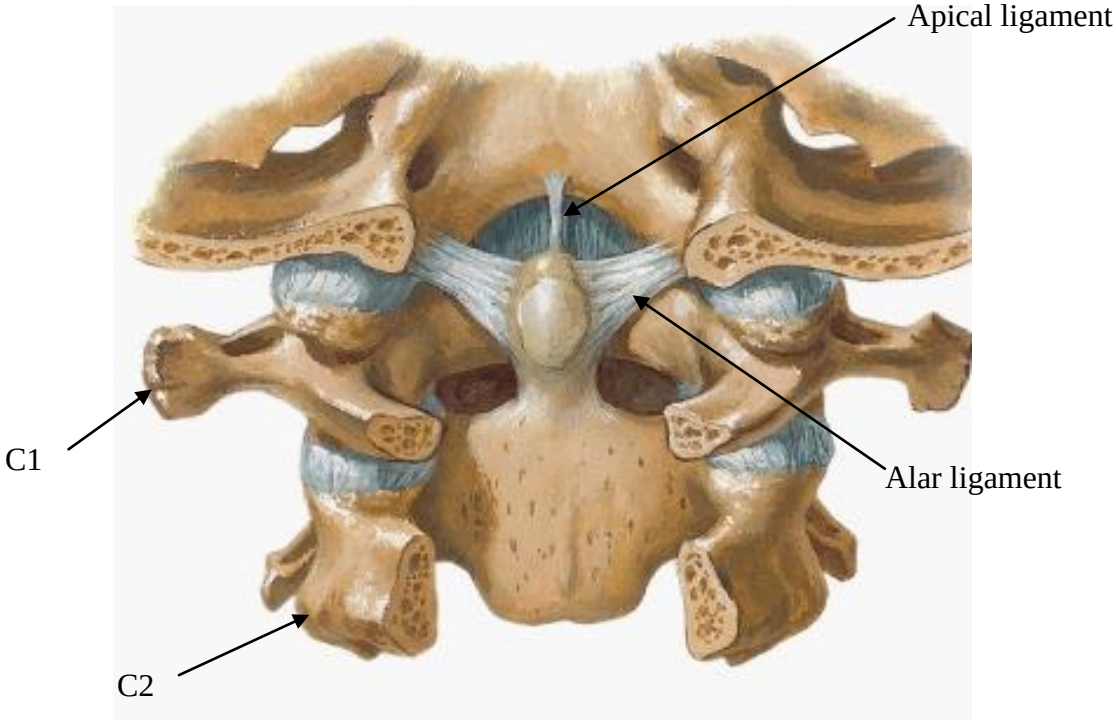

Figure 11: Posterior view of the upper cervical spine with posterior elements and the tectorial and cruciate ligaments removed to show the deepest ligaments [19].

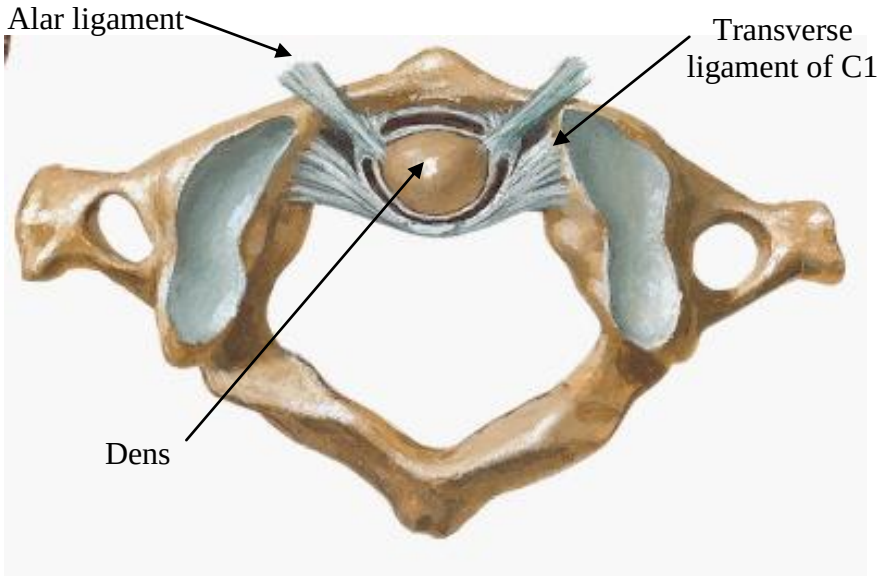

Figure 12: Superior view of the median atlanto-axial joint [19].

Five ligaments strongly influence lower cervical spine behavior. The anterior longitudinal ligament (ALL) is a broad, fibrous band that connects continuously along the anterior aspect of the vertebral column from the sacrum (i.e. tailbone) to C1 with no discrete attachment points (Figure 13) [17]. It helps to limit the neck's range of motion in extension and anterior displacement of the vertebrae [18]. The posterior longitudinal ligament (PLL) is thinner and weaker compared to the ALL and connects from the sacrum to C2 along the posterior aspect of the vertebral column with no discrete attachment points (Figure 9) [17]. It helps to limit the neck's range of motion in flexion and posterior displacement of the vertebrae. The interspinous ligament (ISL) spans the distance between the spinous processes and attaches from the inferior spinous process of one vertebra to the superior spinous process of the adjacent vertebrae, assisting with spine stability [18]. The supraspinous ligament has a similar function and connects from the most posterior end of the spinous process to the posterior end of the adjacent spinous processes. The ligamenta flava run along the laminae and connect the laminae of adjacent vertebrae, limiting neck flexion (Figure 14) [18].

Intervertebral discs lie between adjacent cervical vertebrae, with the exception of the atlanto-occipital and atlanto-axial joints. Intervertebral discs are viscoelastic in nature and support compressive loads within the spine (Figure 14).

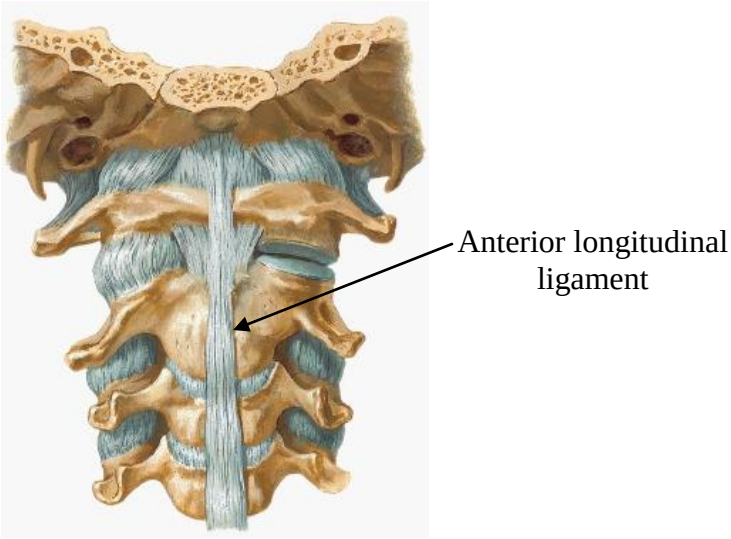

Figure 13: Anterior view of the cervical spine [19].

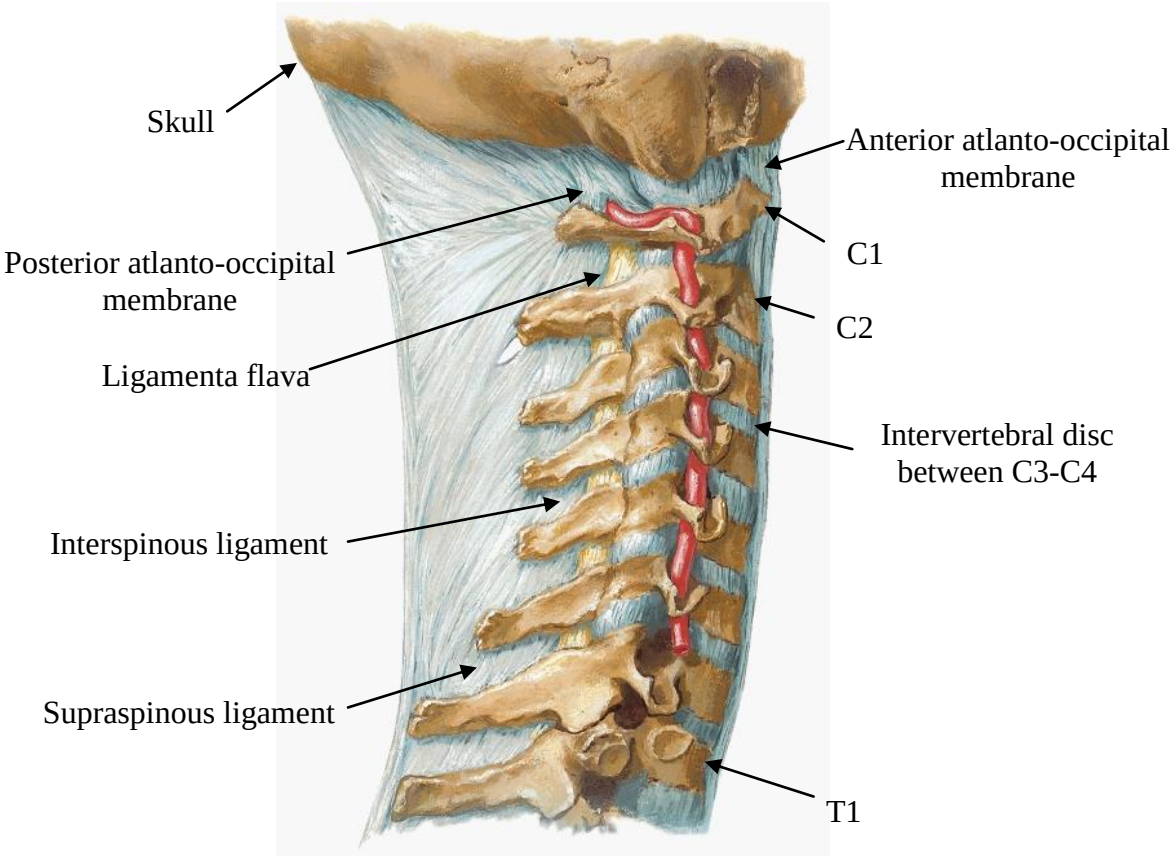

Figure 14: Right lateral view of the cervical spine [19].

Chapter 3

Methods

3.1 Solid Geometry Creation

3.1.1 Vertebrae

As described in the *Modeling Fundamentals* section, accurate geometry is essential to any computer model. For the purposes of this study, solid models were created of the cervical vertebrae, T1, and the skull.

A 3D reconstruction was performed by utilizing a 3D scanner (FaroArm Technologies, Lake Mary, FL) to obtain data from an actual cervical spine specimen. The 3D scanner utilizes a hand-held laser probe that projects a light onto the specimen which is projected back through a sensor (Figure 15). Using triangulation techniques, the probe can calculate its distance from the specimen relative to its internal coordinate system. An external reference, in this case a FaroArm, was then used to relate the data to a global coordinate system.

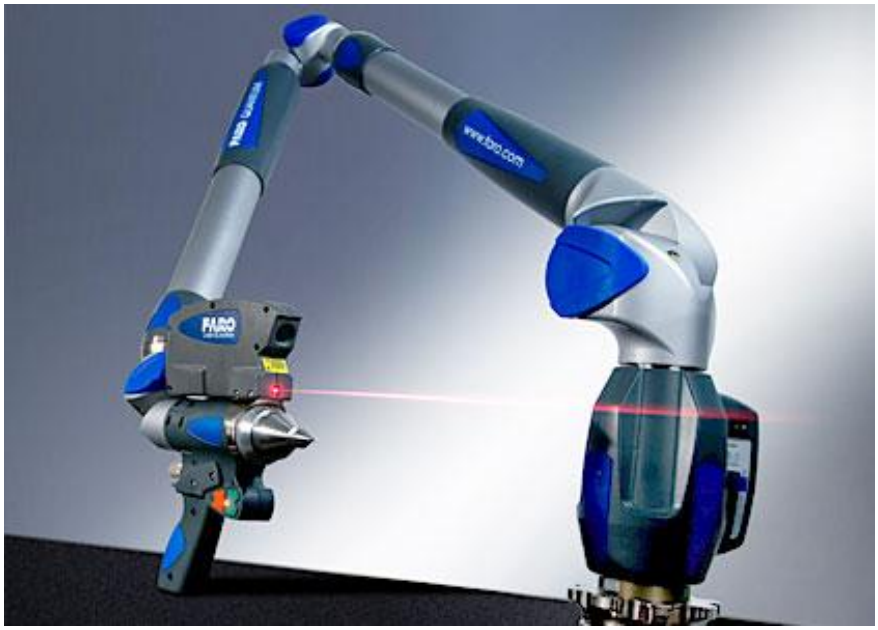

Figure 15: FaroArm with laser attachment (from: http://www.faro.com).

Before a scan, each vertebra was placed on a table covered with black, non-reflective cardboard to reduce unwanted light interference. The scanner was passed over the vertebra, at different orientations, approximately 15 times to obtain a point cloud of geometric samples. Once the exposed half was completely scanned, the vertebra was flipped and the process was repeated. Each hemi-vertebra was saved as a separate data file.

Point cloud data was imported into PolyWorks (InnovMetric, 2010) where data were converted to a polygonal mesh model. In a polygonal mesh model, individual points from the point cloud are connected to form small, flat polygonal surfaces that mesh to represent an object's geometry. A finer mesh produces a smoother contour, more detail, and a more accurate representation. After mesh creation, several functions were used to fix surface blemishes such as holes and intersected polygonal surfaces. Each mesh was exported from PolyWorks as a .stl file type.

For solid model creation, each polygonal mesh was imported into RapidformXOR (Rapidform, 2010). First, the two halves of each scanned vertebra were aligned to form one mesh. This was possible because each polygonal mesh had the same coordinate system defined by the Faro 3D scanner. Once combined, NURBS surfaces were automatically fit over the polygonal mesh. NURBS surfaces use non-uniform, free splines to represent complex geometries. Using software functions, the NURBS surfaces were optimized to best fit the scan data. Once the surfaces were fit, the model was exported as a parasolid CAD file. Figure 16 summarizes the solid geometry creation process.

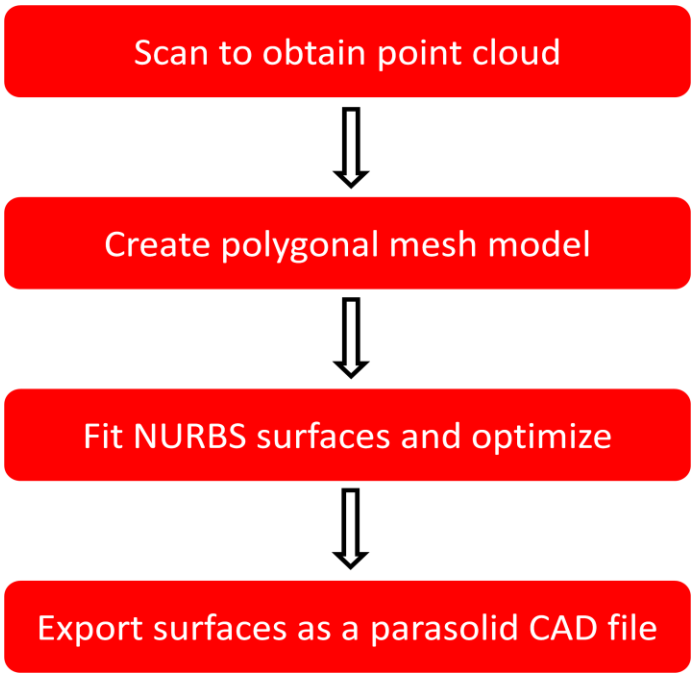

Figure 16: Summary of solid geometry creation.

3.1.2 Skull

The skull used in the model was provided by Greg Knapik and was produced from a CT reconstruction of a rear impact test PMHS. For consistency, the experimental data input to the model was obtained using the same subject. The subject was 87 years old with a weight of 87.3 kg and height of 178 cm. The head weighed 3.7 kg.

The head geometry is different than the vertebrae in that it is modeled as a shell with no volume properties. Because the vertebrae are solid models, mass properties such as center of mass and moment of inertia can be derived numerically. However, the head requires user input for mass and center of mass.

In the CT reconstruction process, certain important features of the skull were lost. The occipital condyles and foramen magnum are not present in the shell. Despite this limitation, their locations can be approximated using the mastoid process (Figure 7).

3.2 Assembling the Cervical Spine

To create a cervical spine model, anatomically correct articulation of the solid bodies is equally important as their geometric accuracy. To achieve this, the vertebrae and skull were oriented to give proper curvature and intervertebral disc spacing as documented in literature.

3.2.1 Lower Cervical Spine

In the lower cervical spine, intervertebral disc spacing was defined using geometric relationships obtained by Gilad and Nissan [20]. In this study, x-rays from 157 healthy, male subjects were analyzed in a standing erect position to obtain the cervical

spine geometric relationships. Table 1 summarizes these results and Figure 17 shows how the results were applied to the model.

Table 1: Geometric relationships for cervical vertebrae (mm) [20].

	a	b	c
	Spinous Process Spacing	**Posterior Disc Spacing**	**Anterior Disc Spacing**
C2-C3	20.5 ± 3.9	3.4 ± 1.0	4.8 ± 1.0
C3-C4	17.5 ± 3.5	3.3 ± 0.9	5.3 ± 0.9
C4-C5	13.1 ± 3.6	3.0 ± 1.0	5.5 ± 1.0
C5-C6	13.8 ± 3.5	3.0 ± 0.9	5.4 ± 1.0
C6-C7	13.8 ± 3.6	3.3 ± 1.0	5.2 ± 1.0
C7-T1	17.4 ± 3.2	3.5 ± 1.2	4.7 ± 1.2

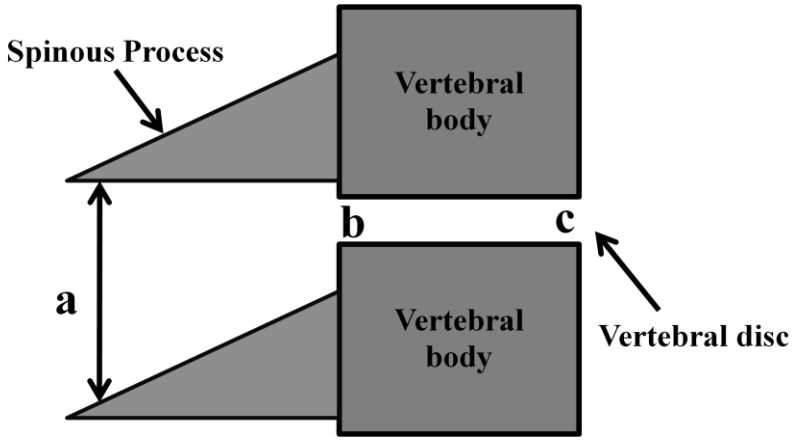

Figure 17: Intervertebral disc spacing schematic; (a) represents the spacing between adjacent spinous processes, (b) represents the posterior disc spacing, and (c) represents the anterior disc spacing applied to the model using published geometric relationships [20] .

Proper cervical spine curvature was defined using previously published cervical lordosis values and facet joint spacing [14]. Both T1 and C7 were oriented with their vertebral bodies rotated 25 degrees counterclockwise when viewed from a left lateral orientation. Moving in the superior direction from C7, each subsequent vertebra was rotated 5 degrees clockwise relative to its inferior vertebra. Facet joint spacing was set to approximately 2.5 mm.

3.2.2 Upper Cervical Spine

Using published cervical lordosis values [14], C1 and C2 were set parallel to the transverse plane. The orientation between C1 and C2 was defined by aligning the articular facet on the anterior surface of the dens with the articular facet on the posterior side of the anterior arch of C1. The orientation between the skull and C1 was defined relative to the posterior aspect of the occipital bone and the mastoid process using anatomical models from text [17]. These features were chosen for orientation because the preferred features on the inferior base of the skull, the occipital condyles and the foramen magnum, were not maintained through 3D reconstruction.

3.3 Rear Impact Cervical Spine Model Development

3.3.1 Overview

To develop the 2D rear impact cervical spine model, the properly articulated spine was constrained with mechanical force elements that represented spinal ligaments and intervertebral discs. Spinal ligaments were modeled as linear spring/damper elements and intervertebral discs were modeled as bushing-like joints defined by shear, axial, and rotational stiffness. The model was simulated by applying T1 kinematics from

experimental data to T1 of the model. The model was validated to evaluate its ability to simulate cervical spine kinematics in low and moderate speed rear impact conditions.

3.3.2 Coordinate System Definition

A Cartesian coordinate system was used for model development. In this coordinate system, +x was directed in the anterior direction, +y was directed in the superior direction, and +z was directed in the right lateral direction (Figure 18).

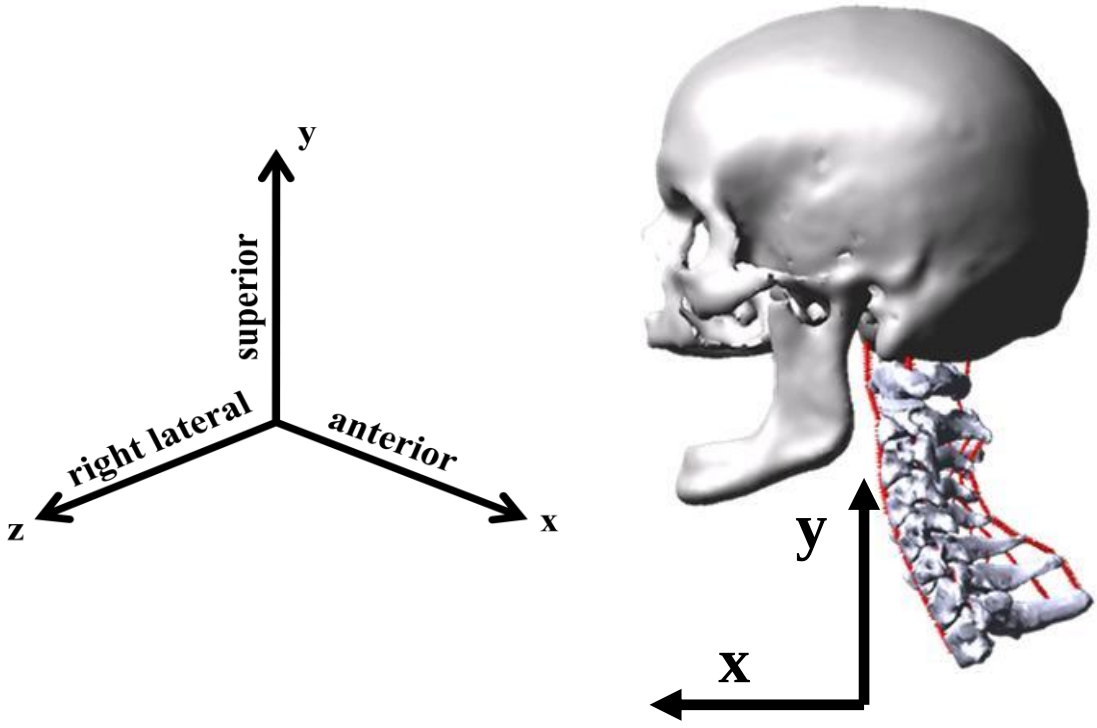

Figure 18: Model coordinate system.

3.3.3 Model Mass Properties

A uniform density of 2g/cm^3 was applied to each vertebra in the model. With this information, ADAMS automatically calculated mass, center of mass, and moment of inertia for each element. Since the skull was a shell with no volume properties, it could

only be defined as a point mass with no moment of inertia. A head mass of 3.7 kg was applied to the model, obtained directly from subject head weight. The center of mass of the skull was defined using values from literature relative to the anatomical reference system used in this study (Figure 19) [21]. Using this coordinate system, the head center of mass was located 2.7 cm in the +y direction and 0.8 cm in the +x.

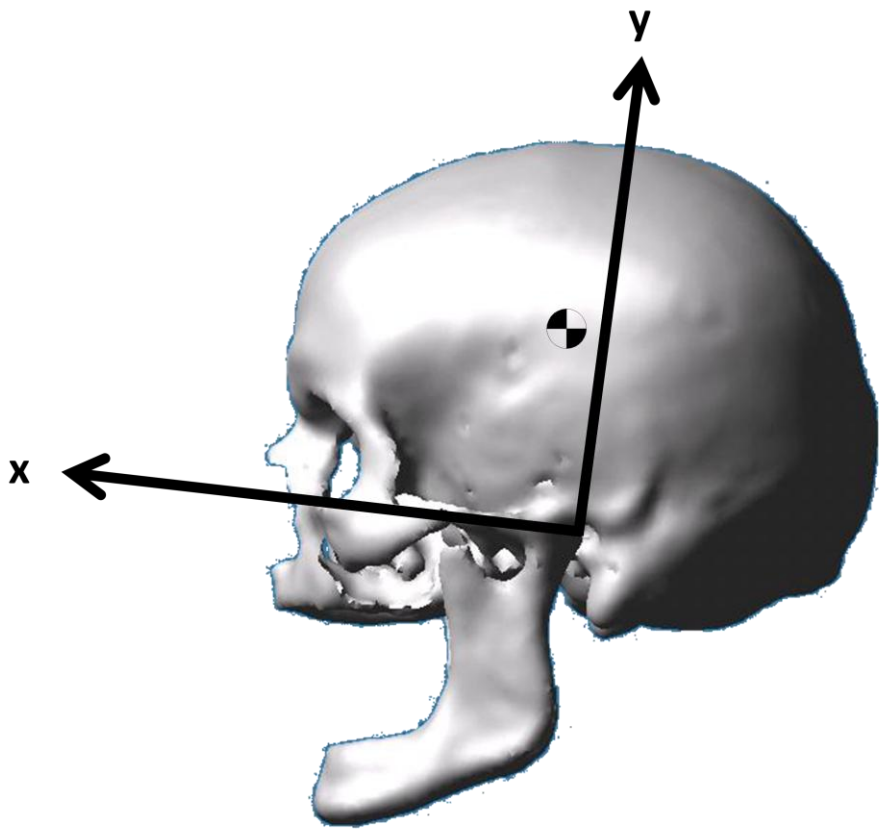

Figure 19: Anatomical reference system of the skull with center of mass.

3.3.4 Ligament Modeling

To constrain the articulated cervical spine, ligaments modeled as linear spring/damper elements were used. Along with stiffness and damping values, a preload was applied to each ligament. Preload values were chosen to maintain static equilibrium of the model after the application of gravity. Attachment points for the ligaments were defined by anatomical features described previously. Approximations for some ligaments, discussed in subsequent sections, were required because the spring/damper elements could only have discrete attachment points.

3.3.4.1 Lower Cervical Spine

In the lower cervical spine, the ALL, PLL, LF, ISL, and SSL were assumed to have the greatest influence on cervical spine kinematics in rear impact collisions. Properties of these ligaments were obtained from a study of 25 cadavers conducted by Yoganandan et al. [22]. In this study, all ligaments and intervertebral discs were transected except for the structure of interest. The vertebral bodies superior and inferior to the test ligament were loaded in tension at a quasi-static rate of 10 mm/s. Stiffness was defined as the slope of the most linear portion of the force-deformation curve.

Table 2 summarizes the results of Yoganandan's study and how those results were applied to the model. In the study, stiffnesses were reported for the C2-C5 and C5-T1 levels. However, because these values were similar, a uniform stiffness average was assumed. These averages were applied to the model with the exception of the ALL and PLL. The stiffnesses of these ligaments were set to 0 because they were already accounted for in the rotational stiffness (flexion/extension) of each intervertebral disc.

This assumption will be explored in the next section. Despite stiffness values being set to 0, these ligaments were still essential to the model because their preload values helped maintain static equilibrium. Also, stiffness of the SSL was not reported so it was assumed to be equal to the ISL stiffness. A damping rate of 2 N-s/mm was applied to every ligament in the model, consistent with the value used by Dauvilliers et al. [15] in their finite element model.

Table 2: Reported and model stiffnesses in the lower cervical spine.

Ligament	+Reported Stiffness (N/mm)	Model Stiffness (N/mm)
ALL	16.7 ± 2.7	0*
PLL	25.4 ± 7.2	0*
ISL	7.74 ± 1.61	7.74
SSL	Not reported	7.74
LF	25 ± 7.04	25

* Accounted for in intervertebral disc rotational stiffness. The ALL and PLL are still included to assist in maintaining static equilibrium of the model.
+Stiffness was defined as the slope of the most linear portion of the force deformation curve from isolated ligament tensile tests at a quasi-static loading rate of 10 mm/s [22]. Stiffness of the SSL was not specified so it was assumed to have the same properties as the ISL.

Several approximations were made for ligament attachments to the solid bodies. In the anatomical cervical spine, several ligaments have multiple attachment points or an attachment band. However, the modeled ligaments could only have single attachment points with one line of action. For example, the ALL and PLL run continuously along each vertebral body and disc; however, separate springs with single attachment points were approximated for the model (Figure 20 a,b). Similarly, the ISL has an attachment band along the spinous process while the LF has an attachment band along the lamina. In the model, the ISL was approximated as a single spring at the midline of the spinous process. The LF was approximated as a single spring at the intersection of the left and

right laminae (Figure 20c), an acceptable approximate because of the 2D nature of the model.

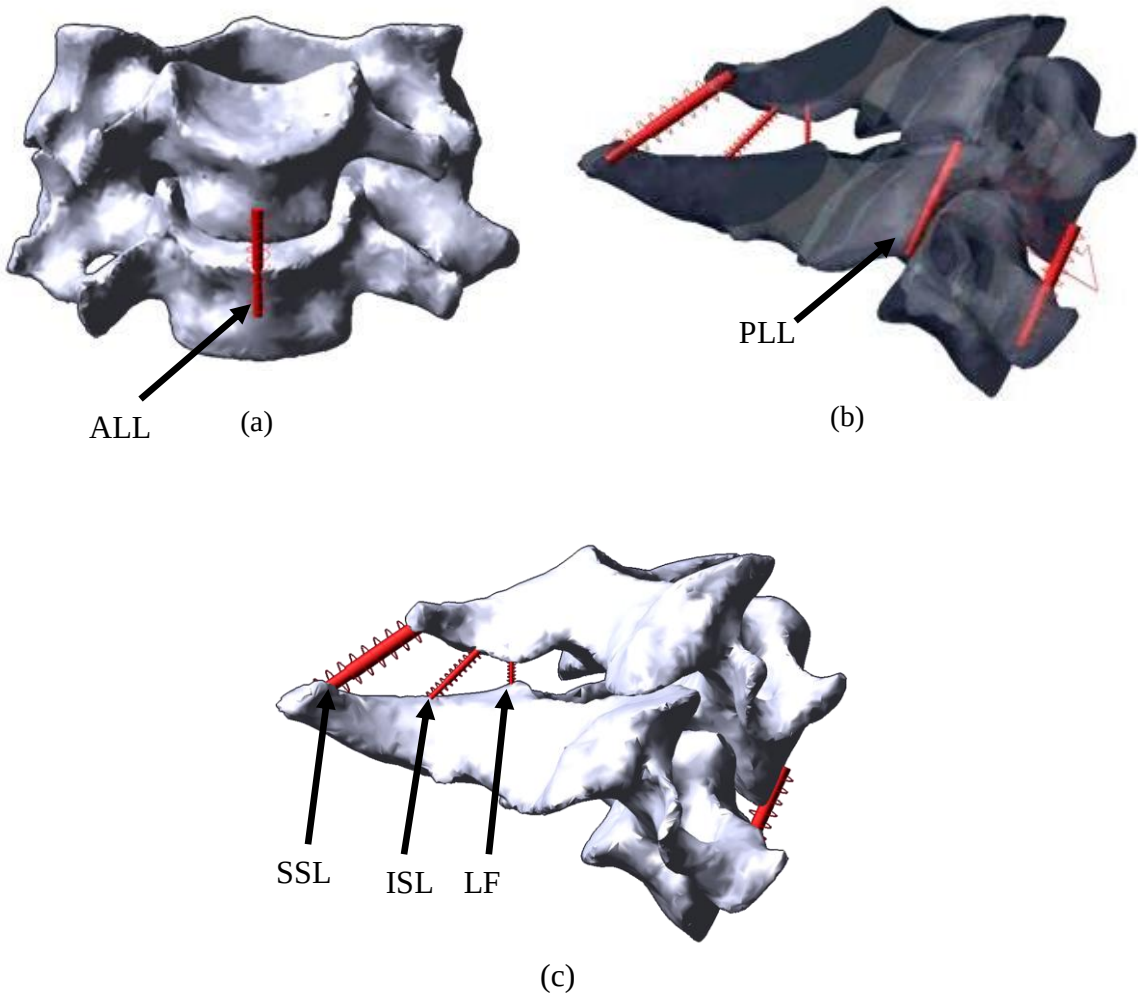

Figure 20: Anterior view (a), right lateral transparent view (b), and right lateral view (c) of C5/C6 unit showing ligament application as single units.

3.3.4.2 Upper Cervical Spine

The upper cervical spine was constrained by several ligaments that attached from the occipital bone (OC) to C1, C1 to C2, and the OC to C2. Properties for these

ligaments were obtained from a previously published review paper written by Yoganandan et al. [7] and were applied appropriately in this model (Table 3).

Table 3: Upper cervical spine ligament properties.

	Ligament	[+]Reported Stiffness (N/mm)	Model Stiffness (N/mm)
OC -> C1	Posterior atlanto-occipital membrane	5.7 ± 0.4	5.7
	Anterior atlanto-occipital membrane	16.9 ± 3.2	16.9
C1 -> C2	Posterior atlanto-axial membrane	Not reported	*5.7
	Anterior atlanto-axial membrane	Not reported	*16.9
	LF	11.6 ± 11.0	11.6
	ALL	24.0 ± 11.7	24.0
	Transverse ligament	Not reported	*25.0
OC -> C2	Tectorial ligament	7.1 ± 2.3	7.1
	Cruciate ligament	19.0 ± 0.2	19.0
	Apical	28.6 ± 29.0	28.6
	Alar	21.2 ± 15.7	21.2

[+]Stiffness properties were obtained from a previously published review paper [7]. The paper did not specify the methods for obtaining the properties.

*Stiffnesses were not reported for the atlanto-axial membrane and the transverse ligament. The atlanto-axial membrane was assumed to have the same stiffness as the atlanto-occipital membrane. The stiffness of the transverse ligament was approximated as an average of the apical and alar ligaments.

Similar to the lower cervical spine, several approximations were made for ligament attachments to the solid bodies. The atlanto-occipital membrane, atlanto-axial membrane, LF, ALL, tectorial ligament, transverse ligament and cruciate ligament were all modeled to have single attachment points (Figure 21 a-d). The cruciate ligament was resolved to have one line of action despite having several lines of action *in vivo*. This was an acceptable assumption because of the 2-D nature of the model. The transverse ligament was approximated by a single line of action running from the posterior articulating surface of the dens to the posterior articulating surface of C1. To simplify the model, several ligaments sharing the same line of action *in vivo* were added to form a single ligament with a combined stiffness (Table 4). Finally, ligament attachment

locations on the OC were approximated, using the vertebral foramen of C1 as a reference, because of the absence of the foramen magnum in the skull model. Figure 21 illustrates the attachment of ligaments in the upper cervical spine.

Table 4: Combined ligaments.

*Combined Ligaments	Combined Stiffness (N/mm)
Posterior atlanto-axial membrane/ALL	29.7
Anterior atlanto-axial membrane/LF	28.5
Tectorial ligament/ Cruciate Ligament	26.1

* Ligaments sharing approximately the same attachment points and lines of action were treated as springs in parallel by adding their stiffnesses.

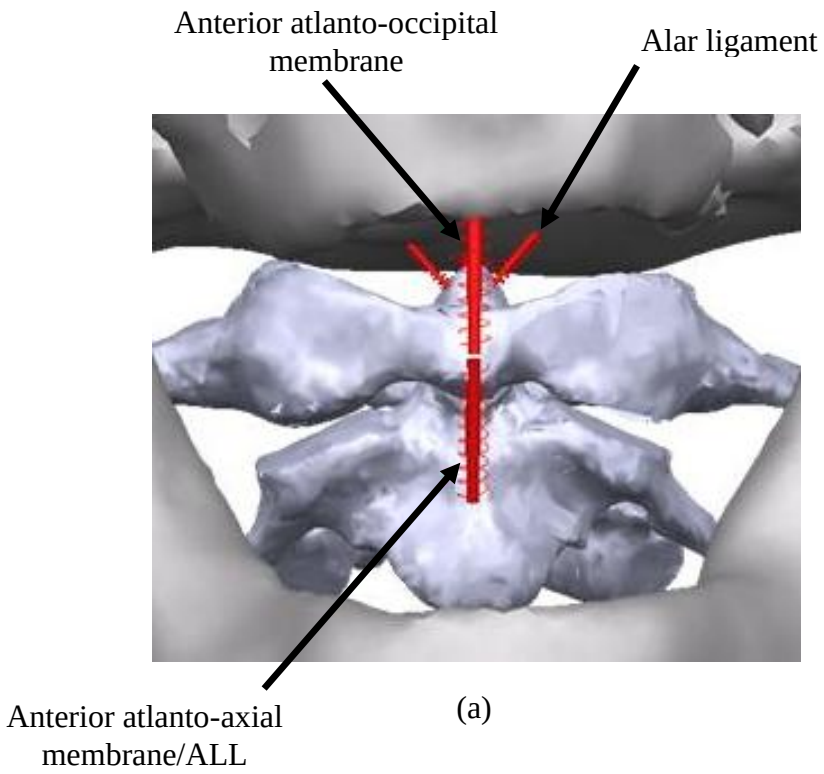

(a)

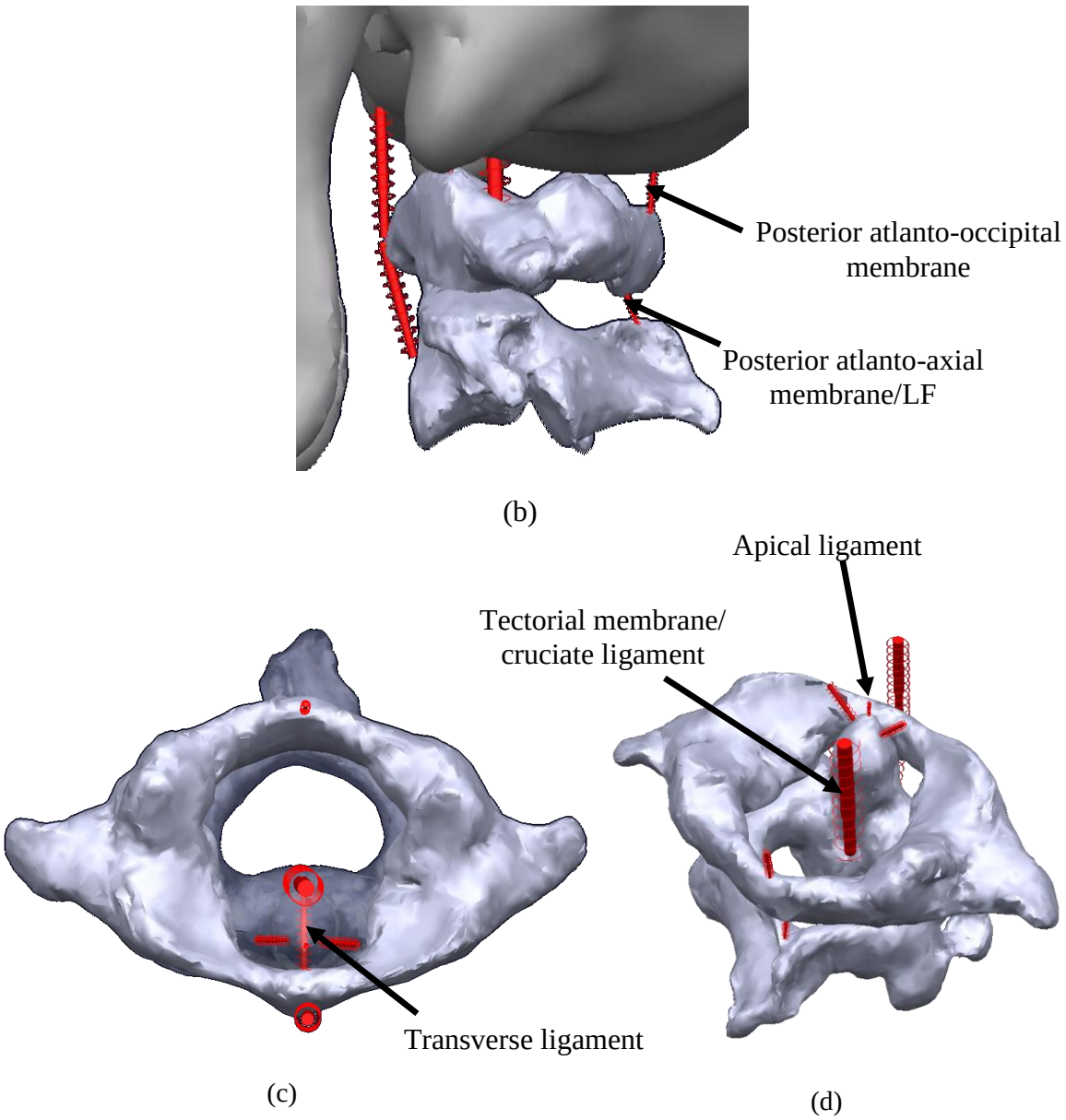

Figure 21: Ligament application in the upper cervical spine; (a) anterior view, (b) left lateral view, (c) superior view, (d) posterior oblique view.

3.3.5 Intervertebral Disc Modeling

Intervertebral discs were modeled as bushing-like joints with axial, shear, and rotational stiffnesses. The modeled discs were placed at every level in the lower cervical spine. The atlanto-occipital and atlanto-axial joints were excluded because intervertebral discs do not exist at those levels. Additionally, a planar joint was placed at each vertebral level to constrain displacement in the z direction and rotation about the x and y axes. These joints constrained the model to be 2-D.

Axial tension properties were obtained from a study that tested isolated disc specimens from cadavers [23]. Each isolated disc specimen consisted of the disc and the inferior and superior vertebral bodies. Specimens were tested to failure; however, the study made no mention of loading rates. Compressive properties were obtained from a review paper written by Yoganandan et al. [7]. However, the source of the data is unknown because the review paper sites it as unpublished data from Yoganandan's laboratory. Shear and rotational stiffness values were obtained from a study that examined disc segments consisting of the disc, the inferior and superior vertebral bodies, the PLL, and the ALL. The inferior vertebral body was fixed in a testing apparatus and static shear and rotational loads were applied to the superior vertebral body [24].

Intervertebral disc properties applied to this model are summarized in Table 5. As mentioned previously, due to the methodology of Moroney's testing, stiffnesses of the ALL and PLL were included in the disc rotational stiffness. Shear stiffness and rotational stiffness were simplified by averaging the coupled motions (i.e. anterior/posterior and

flexion/extension). It is also worth noting that the discs are non-linear and are considerably stiffer in compression than tension.

Table 5: Disc properties applied to the model.

Level	[+]Tension (N/mm)	[+]Compression (N/mm)	[+]Anterior/ Posterior Shear (N/mm)	Flexion/ Extension* (N-mm/deg)
C2-C3	63.5	637.5	55.5	265
C3-C4	69.8	765.3	55.5	265
C4-C5	66.8	784.6	55.5	265
C5-C6	22	800.2	55.5	265
C6-C7	69	829.7	55.5	265
C7-T1	82.2	973.6	55.5	265

*Accounts for ALL and PLL stiffness.

[+]Tensile disc stiffness was obtained from a previously published review paper [7]. Compressive disc stiffness was obtained from isolated disc specimens tested to failure [23]. Shear and rotational stiffness values were obtained from disc segments consisting of the disc, the inferior and superior vertebral bodies, the ALL, and the PLL. The inferior vertebral body was fixed and static shear and rotational loads were applied to the superior vertebral body [24].

3.3.6 Simulation and Validation

After the cervical spine model was constrained, simulations were run with low (17 km/hr, 8.5g) and moderate speed (24 km/hr, 10.5 g) inputs. T1 kinematics (i.e. linear displacements and angular rotations) for both experimental tests were input directly into T1 of the model.

Validation was performed by comparing head kinematics from the experimental testing and model response. Displacements in the x and y directions, angular rotation about the z-axis, linear acceleration in the x and y directions, and angular acceleration about the z-axis of the head center of mass were plotted and evaluated for goodness of fit by visual inspection.

Chapter 4

Results

4.1 Solid Geometry Creation

The results of the solid geometry creation and the original cervical spine specimens are presented in Figures 22 through 29. Figure 30 shows several views of the skull that was modeled as a shell element. It is not presented with the actual specimen because geometry was obtained from a CT scan.

(a) (b)

Figure 22: C1 specimen (a) and solid body (b).

(a)

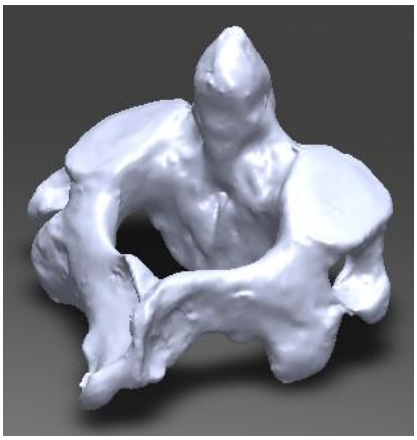

(b)

Figure 23: C2 specimen (a) and solid body (b).

(a)

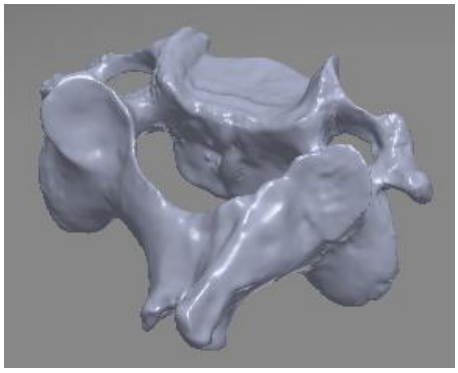

(b)

Figure 24: C3 specimen (a) and solid body (b).

(a)

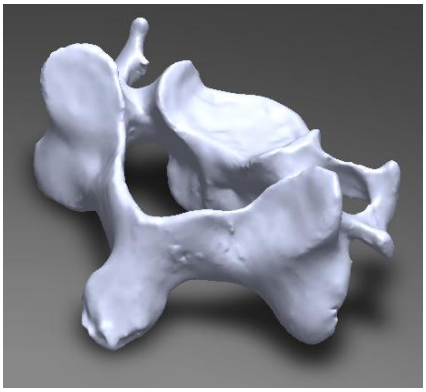

(b)

Figure 25: C4 specimen (a) and solid body (b).

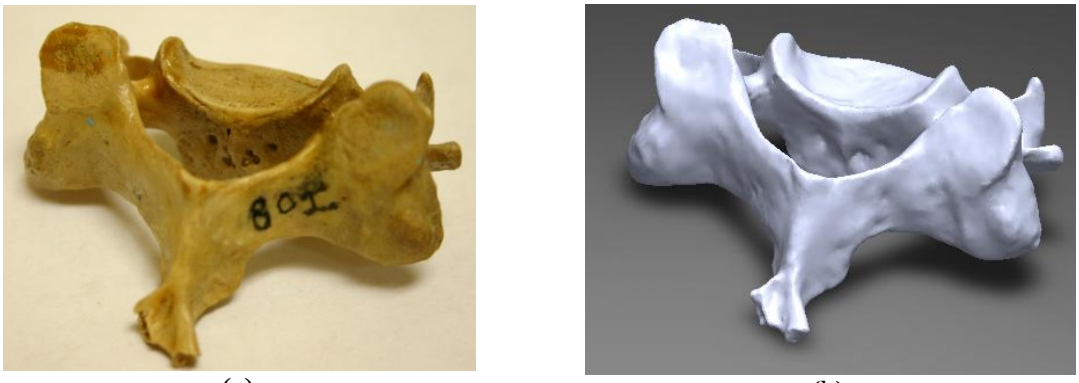

(a) (b)

Figure 26: C5 specimen (a) and solid body (b).

(a) (b)

Figure 27: C6 specimen (a) and solid body (b).

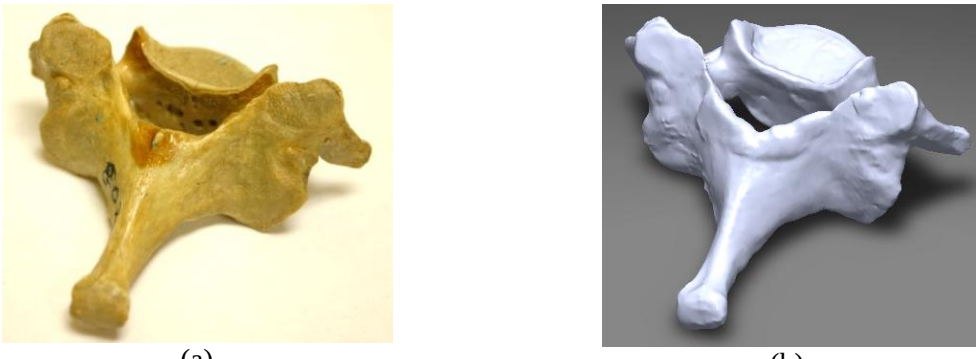

(a) (b)

Figure 28: C7 specimen (a) and solid body (b).

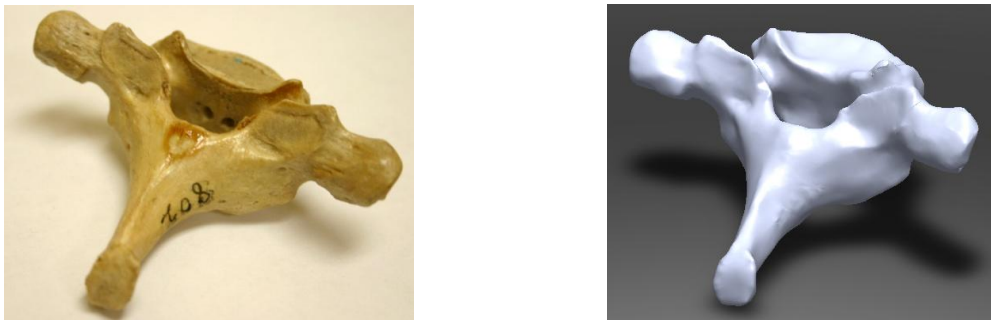

(a) (b)

Figure 29: T1 specimen (a) and solid body (b).

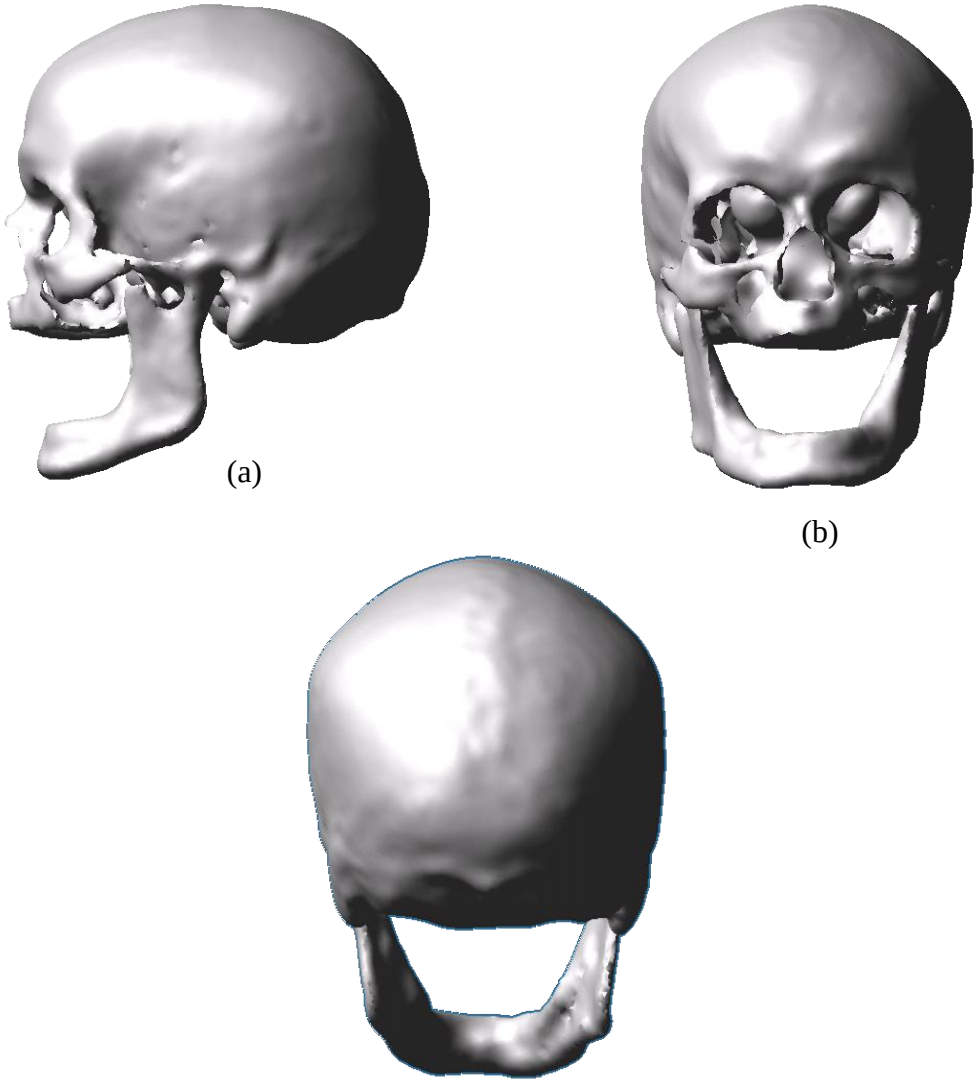

(a) (b) (c)

Figure 30: Left lateral view (a), anterior view (b), and posterior view (c) of skull shell model.

4.2 Properly Articulated and Constrained Cervical Spine

Several views of the articulated cervical spine and head with ligament attachments are shown in Figure 31.

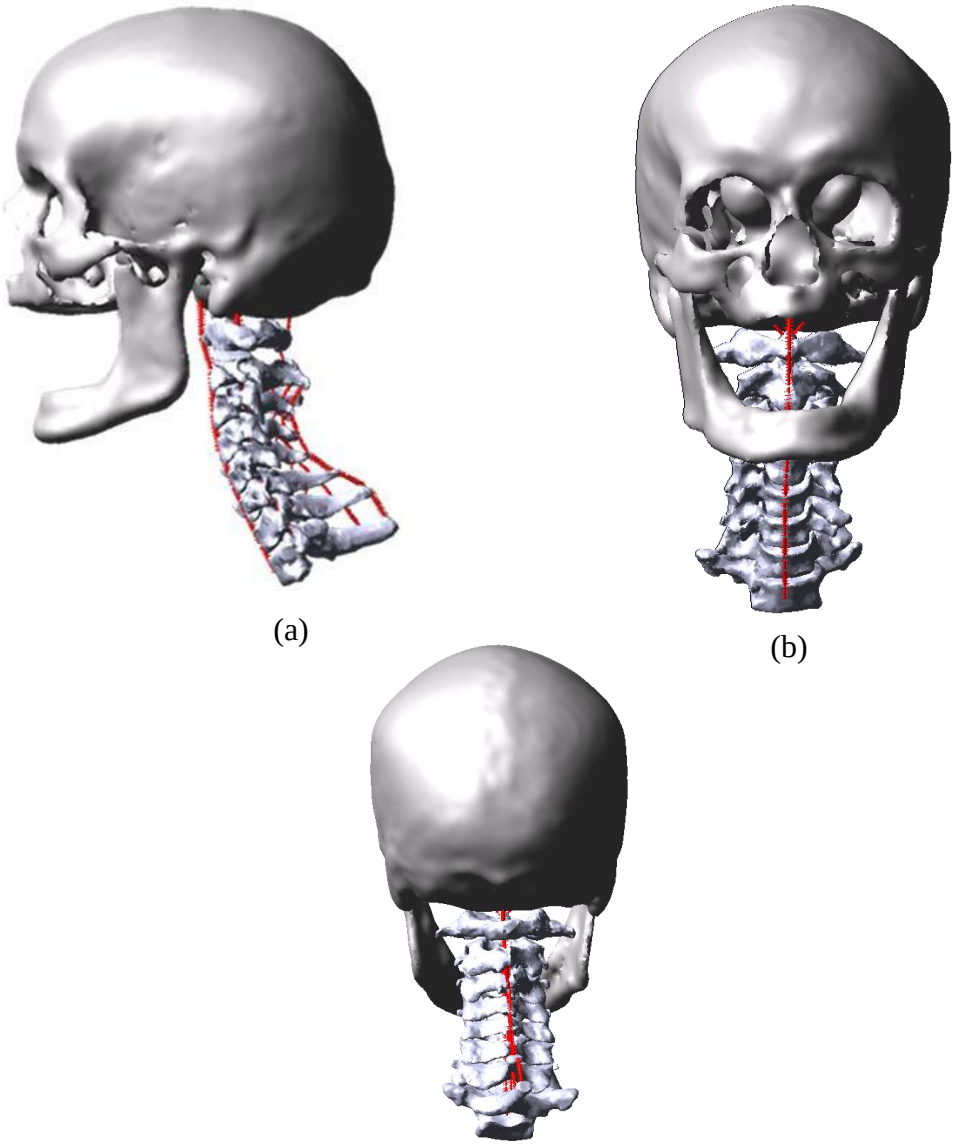

(a) (b) (c)

Figure 31: Articulated cervical spine with ligament attachments; (a) left lateral view, (b) anterior view, (c) posterior view.

4.3 Simulation Results

The simulation results for low and moderate speed inputs, shown at 20 ms increments (with the exception of the final three frames) during the event, are presented in Figures 32 and 33. Results are plotted beyond the point of head contact, 0.118 sec and 0.124 sec in the low and moderate speed simulations, respectively. The figures capture the shape of the cervical spine and head at fixed times; however, the input, T1 kinematics, is not well described. In the experimental rear impact test, an impulse was applied to the massive, high inertia sled. The inertia difference between the sled and thorax caused the thorax to lag. In response to thorax lag, the flexible seatback of the experimental set-up rotated, causing the thorax to travel in the –y direction in addition to the +x direction. The relatively small inertia of the head compared to the thorax caused it to lag in response to the +x displacement of the thorax. Consequently, the cervical spine straightens out before finishing in extension, the expected result of a rear impact collision.

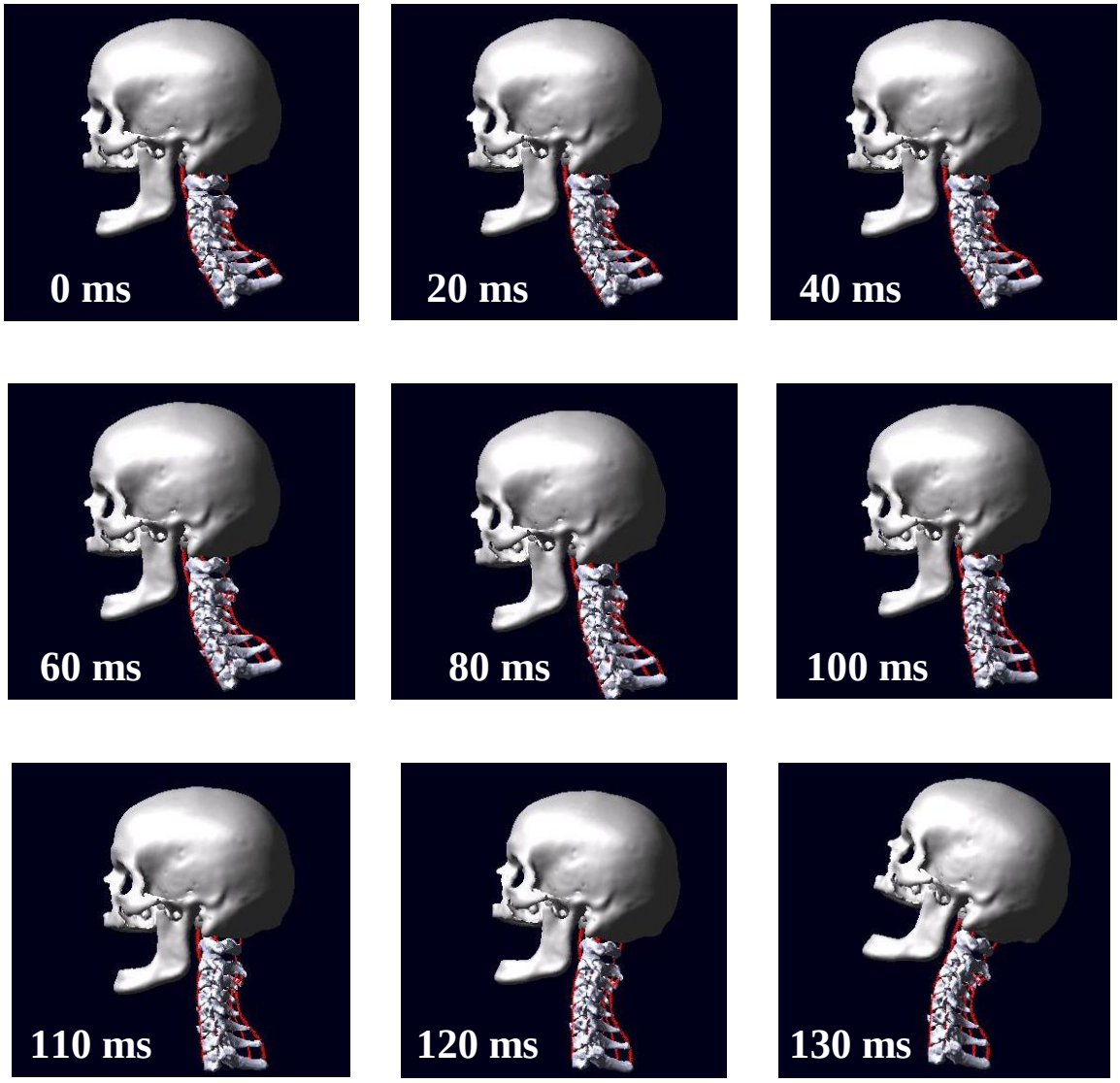

Figure 32: Low speed simulation results shown at 20 ms increments (with the exception of the final three frames). Head contact with the seat head restraint occurs at 0.118 sec.

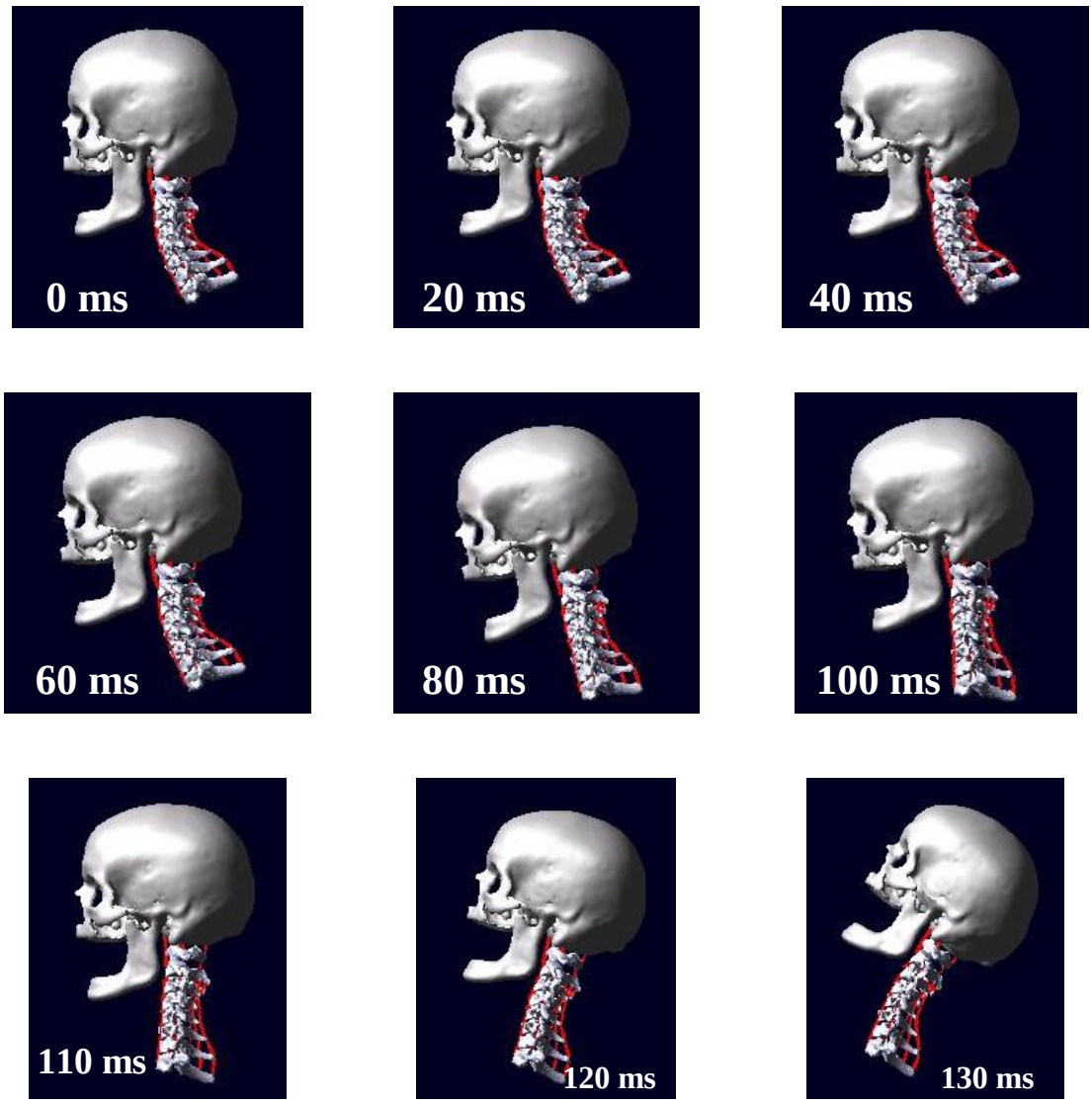

Figure 33: Moderate speed simulation results shown at 20 ms increments (with the exception of the final three frames). Head contact with the seat head restraint occurs at 0.124 sec.

4.4 Validation Results

Figures 34 through 39 present the acceleration validation results for the low and moderate speed simulations. Linear accelerations and angular accelerations of the head

center of mass are plotted for the model and experimental response. The response plots are terminated approximately before the time of head contact with the head restraint of the experimental seat, 0.118 sec.

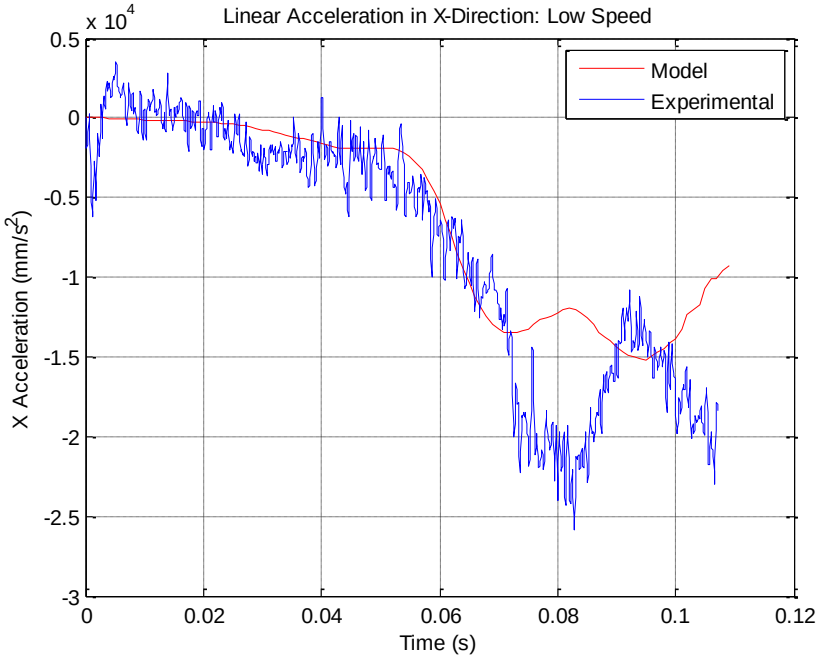

Figure 34: Comparison of model and experimental response: Low speed x linear acceleration of the head center of mass.

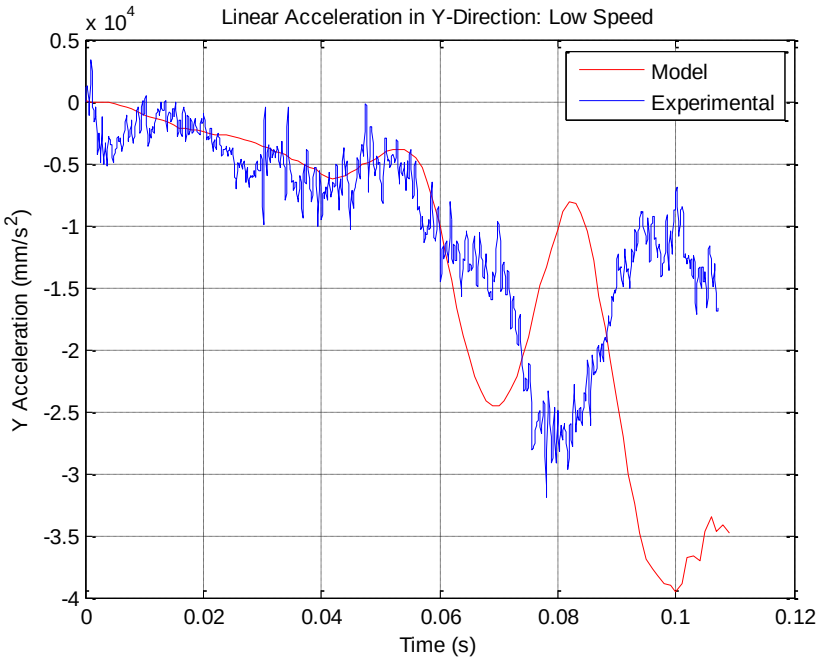

Figure 35: Comparison of model and experimental response: Low speed y linear acceleration of the head center of mass.

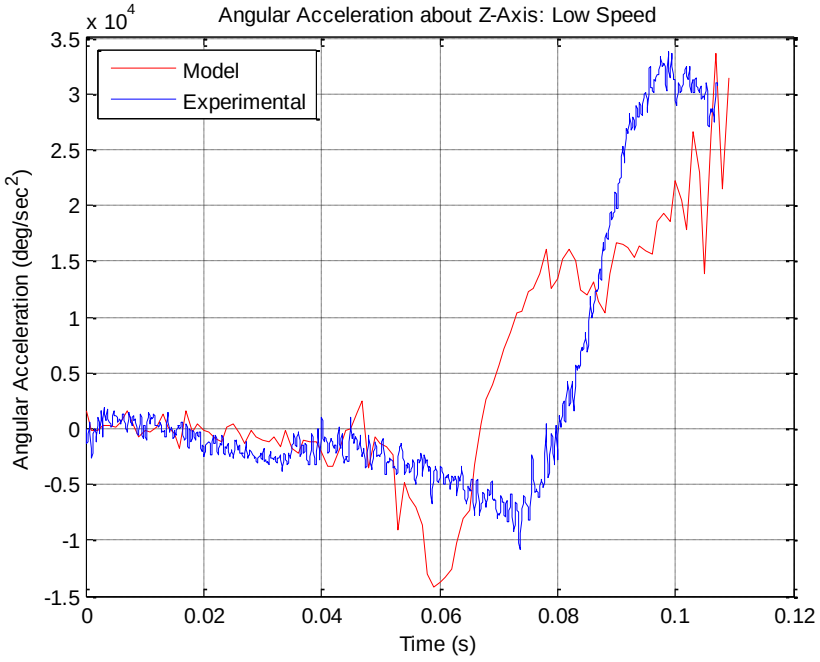

Figure 36: Comparison of model and experimental response: Low speed z-axis angular acceleration of the head center of mass.

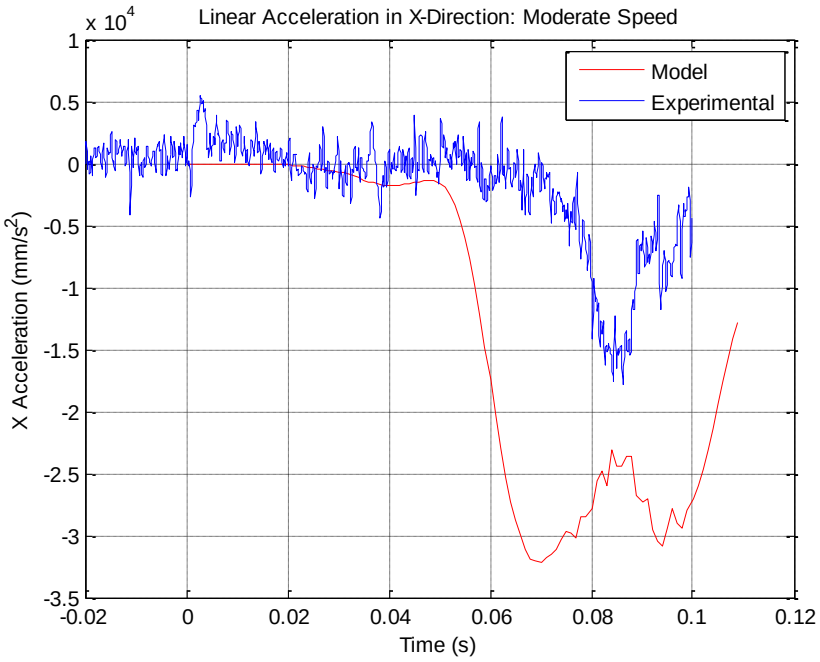

Figure 37: Comparison of model and experimental response: Moderate speed x linear acceleration of the head center of mass.

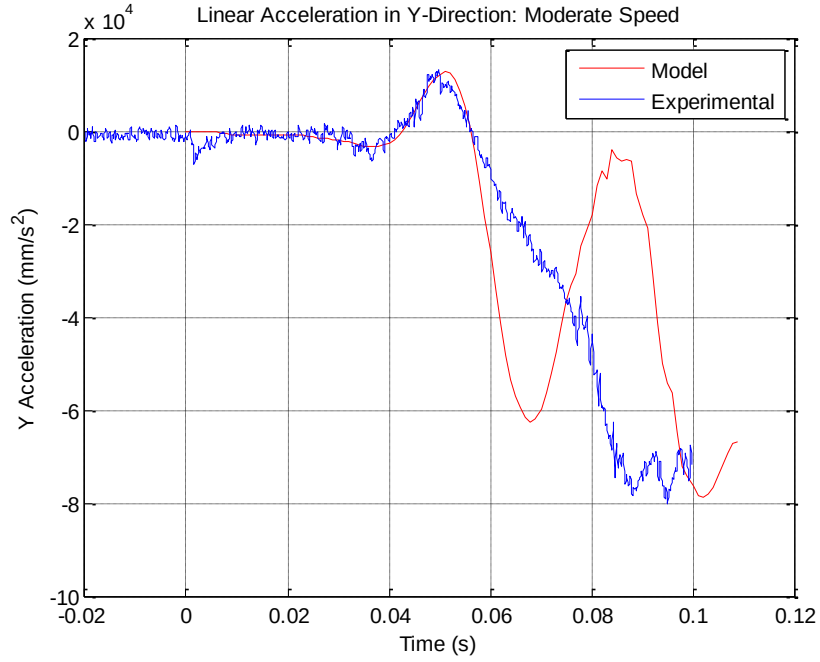

Figure 38: Comparison of model and experimental response: Moderate speed y linear acceleration of the head center of mass.

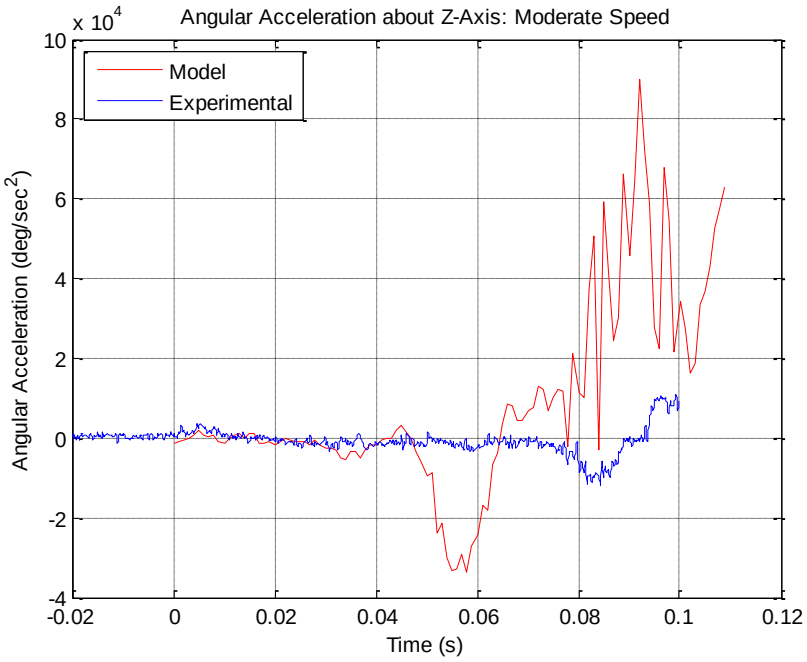

Figure 39: Comparison of model and experimental response: Moderate speed z-axis angular acceleration of the head center of mass.

Using visual inspection, the low speed model responses of Figures 34 through 36 match well with the experimental response except for a ~10 ms lead in model response. In the moderate speed validation (Figures 37 through 39), the error between model and experimental response is much greater. The moderate speed angular acceleration (Figure 39) has extremely large errors and sharp peaks that vary rapidly. Furthermore, the model response lead has increased to approximately 25 ms.

Figures 40 through 45 present the displacement validation results for the low and moderate speed simulations. Linear displacements and angular rotations of the head center of mass are plotted for the model and experimental response. The response plots

are terminated approximately before the time of head contact with the head restraint of the experimental seat, 0.124 sec.

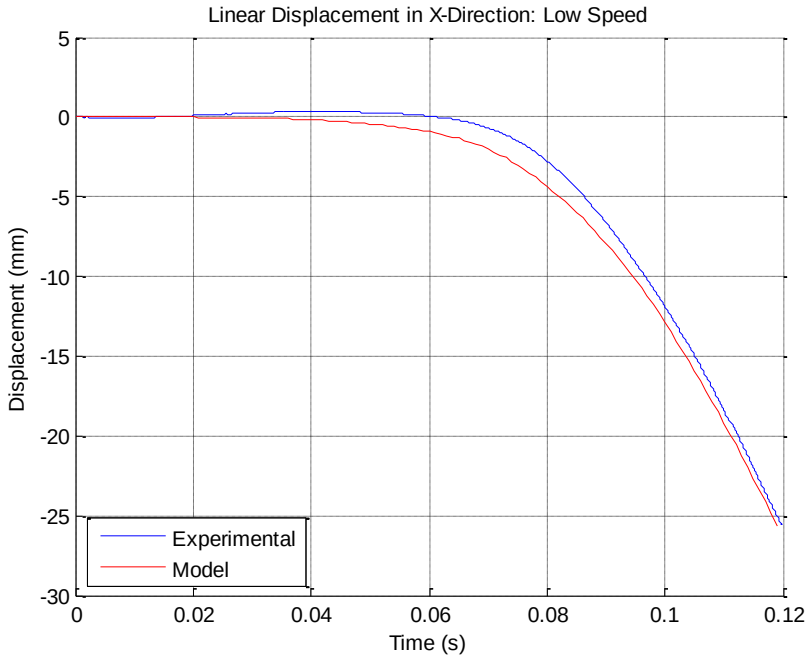

Figure 40: Comparison of model and experimental response: Low speed x linear displacement of the head center of mass.

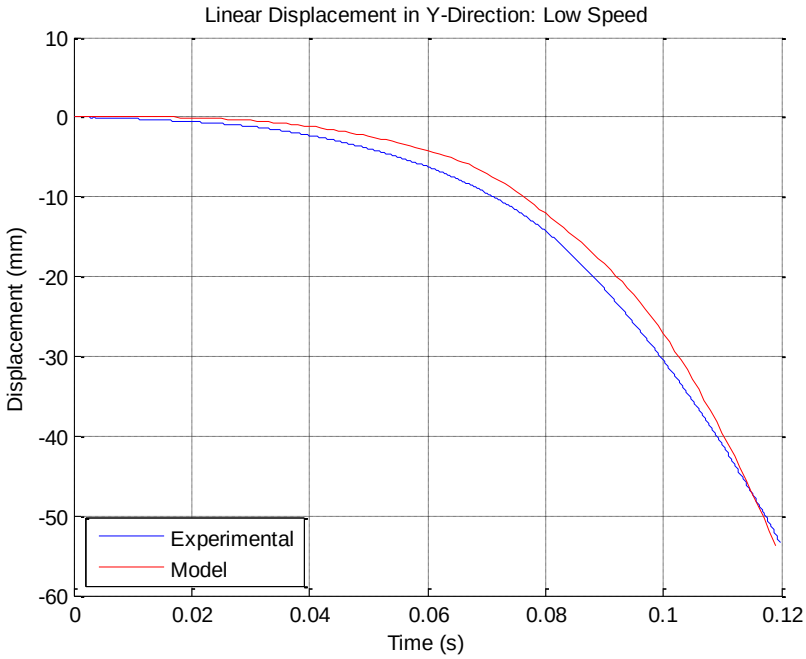

Figure 41: Comparison of model and experimental response: Low speed y linear acceleration.

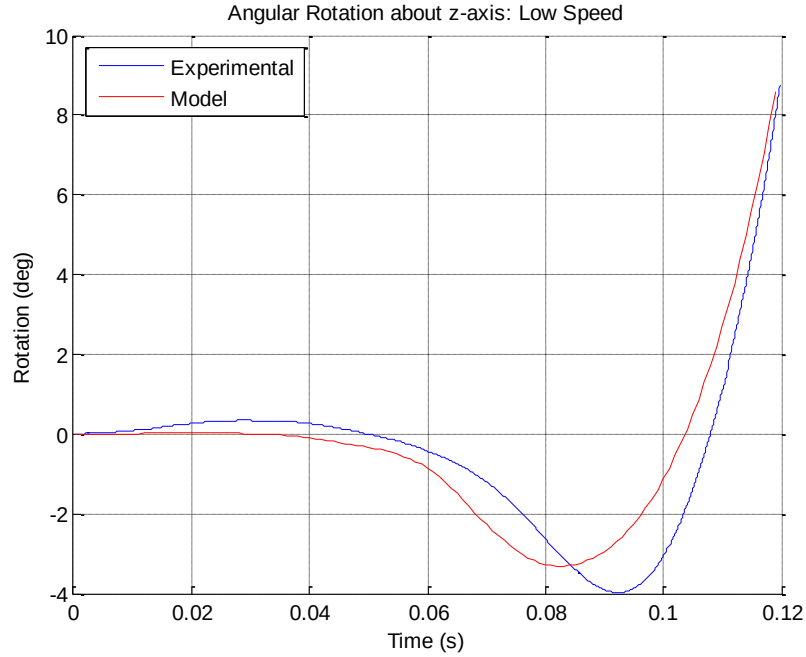

Figure 42: Comparison of model and experimental response: Low speed angular rotation about the z-axis.

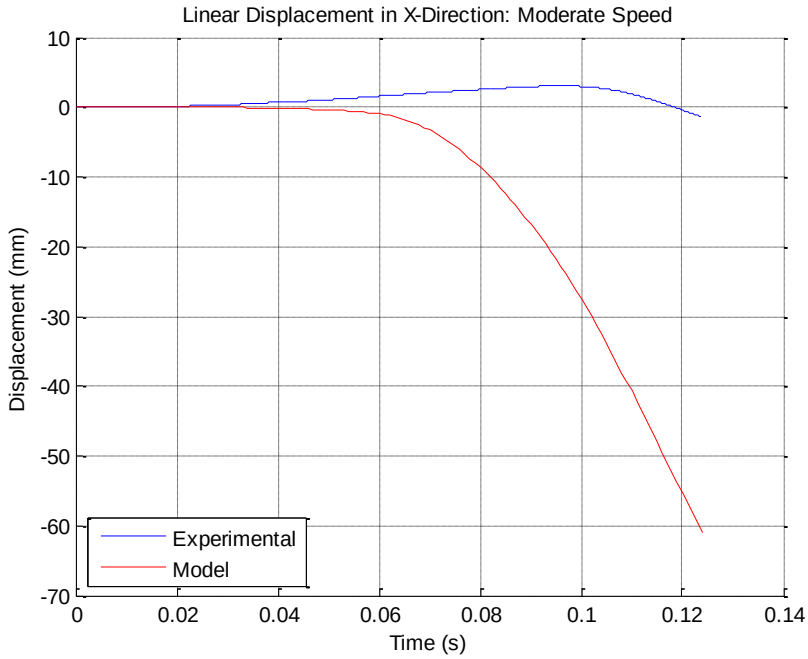

Figure 43: Comparison of model and experimental response: Moderate speed x linear displacement of the head center of mass.

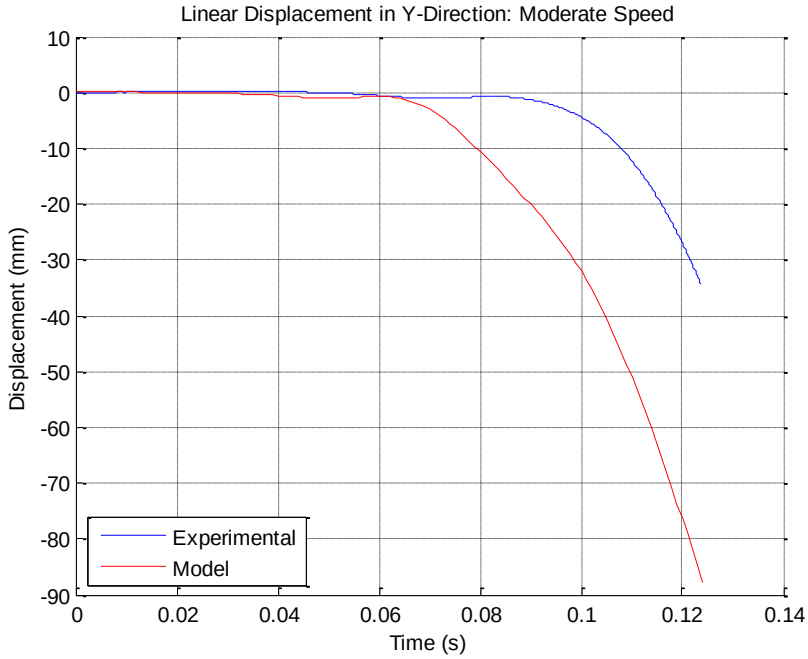

Figure 44: Comparison of model and experimental response: Moderate speed y linear displacement of the head center of mass.

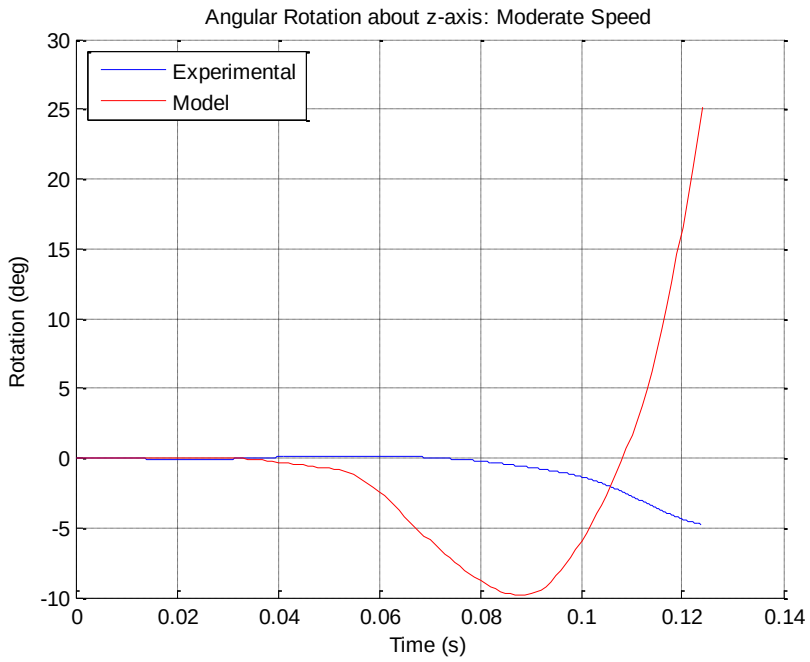

Figure 45: Comparison of model and experimental response: Moderate speed z-axis angular rotation.

In the low speed experimental response, the head displaces in the –x and –y directions because seatback rotation overcomes the +x displacement of the impact sled. The head flexes slightly before finishing in extension. The low speed model predicts these displacements and the rotation extremely well, with the exception of a slight lead in model response angular rotation.

The moderate speed experimental response of the head looks different when compared to the low speed response. The head displaces slightly in the +x direction because the +x displacement of the impact sled overcomes the seatback rotation. Seatback rotation causes –y displacement of the head. The head has little angular rotation before contact with the head restraint.

The moderate speed model responses do a poor job in predicting head displacements and rotation. There is a large amount of error between the model and experimental responses. Furthermore, a large amount of model response lead is seen in displacement and rotation plots.

Chapter 5

Discussion

5.1 Solid Geometry Creation

The modeled solid bodies created in this study (Figures 22 through 30) provide an extremely accurate and useful set of vertebrae for use in dynamic simulations. Fine details in some vertebra (e.g. transverse foramen) were not maintained through 3-D reconstruction; however, these features were not critical to the overall accuracy of the model. All features that influenced mass properties and soft tissue attachment points were modeled with high accuracy. Accurate solid bodies were important for two reasons. 1) Dynamic simulations require mass properties such as center of mass and moment of inertia, and the solid geometry allowed for automatic and accurate mass property computations to be done by ADAMS, and 2) Maintaining the characteristic shape of the vertebrae provided anatomical landmarks for the attachment of the ligaments and discs.

The 3-D reconstruction process utilized two software packages, PolyWorks and RapidformXOR, however, the process was somewhat redundant. Originally, the project planned to use PolyWorks for point cloud acquisition and post processing. PolyWorks was used successfully for all point cloud acquisitions; however, challenges

were faced when attempting to use it for post processing. The geometry of each vertebra was too complex for the algorithms available in PolyWorks. After several attempts with no results, post processing attempts were transferred to RapidformXOR. In future trials, it is recommended that RapidformXOR be used for point cloud acquisition and post-processing.

Several steps can be taken to ensure optimal point cloud acquisition to assist with post processing. Since the hand held laser scanner utilizes light reflection and triangulation to create a point cloud, any extraneous light sources should be eliminated. It is recommended that the specimens are placed on a dark, non-reflective surface. Furthermore, if the specimen surfaces are reflective, they should be coated with powder to dull the surface.

5.2 Validation

The presence of error and model response lead in the acceleration and displacement plots could result from several sources including approximations and assumptions used in modeling. First, the model approximated ligaments to be linear elements. In reality, ligaments have non-linear properties and get stiffer when elongated. Ligaments are, however, linear at low displacements. It is possible that the ligament displacements seen in the low speed response stayed within the linear range. This would explain the improved results of the low speed response compared to moderate speed. Second, ligaments are viscoelastic materials that have high rate dependence. The properties applied to the ligaments and discs were limited to previously published values. Each source investigated ligament properties under static or quasi-static loading. Yet,

these same properties were applied to low and moderate speed whiplash models which involve high strain rates which are not near static or quasi-static levels. Third, soft tissues vary greatly from subject to subject. However, this validation compared the results of a model developed from literature to a single subject with unique anatomy and assumedly unique soft tissue material properties. Fourth, several elements of the cervical spine were omitted in modeling to reduce model complexity or because their properties were not well defined in literature. The subsequent section will identify some of those elements. Finally, the model assumed the head to be a point mass, yet in reality the head is a distributed mass with an uneven profile. Assuming the head as a point mass could lead to kinematic errors in the simulation.

5.3 Model Limitations

The model developed in this study is limited in that it does not model the non-linearities of the ligaments, nor does it fully capture their viscoelastic nature. Furthermore, certain elements were omitted from the model to reduce complexity or because sufficient information was lacking in the literature to model the element. Model complexity was reduced by omitting the articulation of the facet joints, and by omitting the passive influence of muscle and the inertia it adds to the system. The nuchal ligament is important for cervical spine biomechanics; however, it was not included from the model because its properties were not documented in literature. Similarly, information was lacking for the viscoelastic behavior of the discs and the articulation of the atlanto-axial and atlanto-occipital joints, so these aspects were omitted as well. Finally, the head was modeled as a point mass when in reality it has distributed mass with an uneven profile.

5.4 Future Work

Future work should focus on addressing the limitations of the previous model. More specifically, future models should include non-linear elements, consider the viscoelastic nature of soft tissues, include elements omitted from the initial model, and improve the model of the head to have better mass properties.

An effort should also be made to optimize the model design variables. An error function between the model and experimental response could be defined. Using optimization algorithms in ADAMS, the design variables could be optimized to minimize the error function and give a better fit between the two responses. To reduce computational time, a sensitivity analysis could be performed to identify the variables which have the greatest influence on the output response.

Chapter 6

Conclusions

- A 2-D rear impact cervical spine model was developed in ADAMS using linear spring/damper constraints and non-linear discs.
- Low speed simulation acceleration results matched well with experimental data except for a ~10 ms lead in model response.
- Low speed head displacement and rotation results matched extremely well with experimental data with the exception of a slight lead in model angular rotation response.
- Moderate speed simulation acceleration results had more error and an approximate lead of 25 ms in model response. The moderate speed model poorly predicted head displacements and angular rotations.
- The error and lead in model response could be the result of using linear instead of non-linear elements, the limited application of viscoelastic properties to modeled soft tissues, the large variation in each subject's soft tissue properties, the omission of some cervical spine elements, and the approximation of the head as a point mass.

- Future work needs to focus on the addition of non-linear elements, improving model rate dependence, the addition of elements omitted from the initial modeling attempt, improving head mass properties, and optimization of design variables.

References Cited

[1] NHTSA, 2007. Motor Vehicle Traffic Crash Fatality Counts and Estimates of People Injured for 2006. NHTSA's National center for statistics & analysis, DOT HS 810 837.

[2] FMVSS 202 Final Rule, 69 FR 74848, December 2004.

[3] Viano, D. C. "Seat properties affecting neck responses in rear crashes: A reason why whiplash has increased." *Traffic Injury Prevention* 4.4 (2003): 214-227.

[4] Bogduk, Nikolai. "An Overview of Whiplash." *Frontiers in Whiplash Trauma*. Eds. N. Yoganandan and F.A. Pintar. Washington, D.C.: IOS Press, 2000. 3-9.

[5] Pike, Jeffrey A. "Whiplash Injury and Vehicle Design Concepts." *Frontiers in Whiplash Trauma*. Eds. N. Yoganandan and F.A. Pintar. Washington, D.C.: IOS Press, 2000. 41-44.

[6] Panjabi, M.M., Ito, S., Ivancic, P., Rubin, W. "Evaluation of the intervertebral neck injury criterion using simulated rear impacts." *Journal of Biomechanics* 38.8 (2005): 1694-701.

[7] Yoganandan, N., Kumaresan, S., Pintar, F. "Biomechanics of the cervical spine Part 2. Cervical spine soft tissue responses and biomechanical modeling." *Clinical Biomechanics* 16.1 (2001): 1-27.

[8] Deng, B., Begeman, P. C., Yang, K. H., Tashman, S., King, A. I. "Kinematics of human cadaver cervical spine during low speed rear-end impacts." *44th Stapp Car Crash Conference* SAE Paper No. 2000-01-SC13 (2000): 171-188.

[9] Panjabi, M.M., Cholewicki, J., Nibu, K., Babat, L.B., Dvorak, J. "Simulation of Whiplash Trauma Using Whole Cervical Spine Specimens." *Spine* 23 (1998): 17-24.

[10] Panjabi, M.M., Ito, S., Ivancic, P., Rubin, W. "Evaluation of the intervertebral neck injury criterion using simulated rear impacts." *Journal of Biomechanics* 38 (2005): 1694-1701.

[11] Yoganandan, N., Pintar, F., Stemper, B., Schlick, M., Philippens, M., Wismans, J. "Biomechanics of human occupants in simulated rear crashes: Documentation of neck injuries and comparison of injury criteria." *44th Stapp Car Crash Conference* SAE Paper No. 2001-01-SC14 (2000). 189-204.

[12] Bertholon, N., Robin, S., J.Y. Le Coz, Potier, P.,Lassau, J.P., Skalli, W. "Human head and cervical spine behaviour during low-speed rear-end impacts: PMHS sled tests with a rigid seat." *IRCOBI Conference 2000*: 265-277.

[13] Yoganandan, N., Kumaresan, S., Voo, L., Pintar, F. "Finite Element Applications in Human Cervical Spine Modeling." *Spine* 21.15 (1996): 1824-1834.

[14] Kleinberger, M. "Application of Finite Element Techniques to the Study of Cervical Spine Mechanics." *37th Stapp Car Crash Conference* SAE Paper No. 933131 (1993): 261-272.

[15] Dauvilliers, F., Bendjellal, F., Weiss, M., Lavaste, F., Tarriere, C. "Development of a Finite Element Model of the Neck." *38th Stapp Car Crash Conference* SAE Paper No. 942210 (1994): 77-91.

[16] Yang, K., Zhu, F., Luan, F., Zhao, L., Begeman, P. "Development of a Finite Element Model of the Human Neck." *42nd Stapp Car Crash Conference* SAE Paper No. 983157 (1998): 1-11.

[17] Moore, K., Agur, A. *Essential Clinical Anatomy*. Philadelphia: Lippincott Williams & Wilkins, 1995.

[18] Hamill, J., Knutzen, K. *Biomechanical Basis of Human Movement*. Philadelphia: Lippincott Williams & Wilkins, 2009.

[19] Netter, F., M.D., *Atlast of Human Anatomy*. Philadelphia: Saunders Elsevier, 2006. Print.

[20] Gilad, I., Nissan, M. "A study of the vertebra and disc geometric relations of the human cervical and lumbar spine." *Spine* 11.2 (1986): 154- 157.

[21] Albery, C. Whitestone, J. Schuck, M., A Comparison of Cadaveric Human Head Masses, Centers of Gravity and Moments of Inertia: Direct Measurement vs. Computed Tomographic Calculation, Presented at the Aerospace Medical Association (AsMA) Annual Scientific Meeting, May 2003.

[22] Yoganandan, N., Kumaresan, S., Pintar, F. "Geometric and mechanical properties of human cervical spine ligaments." *Journal of Biomechanical Engineering* 122 (2000): 623- 629.

[23] Yoganandan, N., Pintar, F., Maiman, D., Cusick, J., Sances Jr. A., Walsh, P. "Human head-neck biomechanics under axial tension." *Medical Engineering & Physics* 18 (1996): 289-294.

[24] Moroney, S., Schultz, A., Miller, J., Andersson, G. "Load-displacement properties of lower cervical spine motion segments." *Journal of Biomechanics* 21.9 (1988): 769-779.